



**UiT** The Arctic University of Norway

The Faculty of Health Sciences

**Polarization of primary human renal proximal tubular epithelial cells  
– a pilot study**

Elias Myrvoll Lorentzen

MED-3950 Master's thesis in medicine – September 2020



## Preface

Som forskerlinjestudent har jeg de siste årene forsket på replikasjonszyklusen til BK Polyomavirus i nyreepitelceller. I forbindelse med dette arbeidet har forskergruppen jeg er en del av sett behovet for en polarisert cellekulturmodell av nyreepitelceller. Det er forsket svært lite på BK Polyomavirus i slike modeller og vi bestemte oss derfor for å utvikle en slik modell. De første pilotforsøkene jeg utførte på polarisering av nyreepitelceller i cellekultur er blitt til denne masteroppgaven. Etter pilotforsøkene har jeg fortsatt arbeidet med nyreepitelcellemodellen og jeg planlegger å bruke den i min videre forskning og i mitt fremtidige doktorgradsarbeid.

Prosesen og arbeidet med modellen har vært svært lærerik og jeg har tilegnet meg nyttig kunnskap om nyreceller, cellebiologi og cellekulturmodeller. Dette vil komme til nytte i mitt videre forskningsarbeid.

Prosjektet varte fra oktober 2018 til august 2019. Forbruksmateriell og celler ble dekt av Avdeling for Mikrobiologi og Smittevern ved UNN. Prosjektet har ikke mottatt ekstern finansiering.

Jeg vil takke min hovedveileder, Christine Hanssen Rinaldo, for svært god veiledning med laboratoriearbeid, metodevalg og skriving av oppgaven. Videre vil jeg takke henne for at hun oppmuntrer og hjelper meg til å forfølge egne ideer i mitt forskningsarbeid. Jeg vil også takke min biveileder, Stian Henriksen, for uvurderlig hjelp og opplæring på lab samt for hans tålmodige og konstruktive tilbakemeldinger. Takk til Randi Olsen og Augusta H. A. Sundbø på Kjernefasiliteten for Avansert Mikroskopi for preparering av prøver til elektronmikroskopi og hjelp med billedtaking. Takk til Øyvind og Håkon på «the lab» for good times. Avslutningsvis vil jeg takke samboeren min Isabell for at du alltid er der for meg.

Tromsø 30.08.20

Elias Myrvoll Lorentzen



# Table of contents

Preface.....	I
Abstract .....	V
Abbreviations .....	VI
Introduction.....	1
Polarized epithelial cells.....	1
Markers of polarity.....	2
Functionality of polarized cells.....	5
Epithelial cells and cell lines for polarization studies.....	6
Epithelial cell culture models .....	7
BK Polyomavirus research lacks a polarized cell model.....	9
Aim .....	11
Material and methods.....	12
Materials and cells.....	12
Virus.....	12
Isolation of cells from urine .....	12
Collagen coating of permeable supports .....	12
Polarization.....	13
Culture of cells in chamber slides.....	13
Transmission and scanning electron microscopy .....	13
Immunofluorescence microscopy .....	14

BKPyV-infections .....	15
Results .....	15
RPTECs from different commercial sources exhibit different ultrastructural morphology.	15
Differentiate leads to increased expression of the tight junction protein ZO-1.....	16
Differentiation leads to apical-basolateral polarity .....	16
RPTECs develop primary cilia .....	17
RPTECs seeded upside-down develop the same morphology .....	18
RPTEC/TERT1 polarize on permeable supports .....	18
Permeable supports are not necessary for polarization of RPTECs.....	19
Cells isolated from urine are similar to commercial RPTECs .....	19
Urinary cells polarize on permeable supports inserts .....	20
Polarized RPTECs are permissive to BK Polyomavirus infection .....	20
Discussion .....	20
Conclusions.....	23
References.....	25
Illustrations and figures.....	34
Grade schemas .....	57

## Abstract

**Introduction:** Epithelial cells are specialized cells with an apicobasal polarity that allows them to exert their functions, such as acting as a barrier and controlling flow and transport of molecules across the epithelial layer. Polarized epithelial cell models have been developed for several organs and yield a more in vivo-like organization than cell monolayers.

BK Polyomavirus (BKPyV) is a ubiquitous virus that infects polarized epithelial cells in the reno-urinary tract. High-level replication in these cells may cause severe disease. Much research has been done on BKPyV, but the majority of studies on BKPyV have been done in non-polarized epithelial cell culture models. We therefore chose to develop a polarized renal cell culture model for assessing the replication cycle of BKPyV.

**Materials and methods:** Adult and fetal human primary renal proximal tubule epithelial cells (RPTECs), immortalized RPTECs and urinary cells were seeded on collagen-coated permeable supports and allowed to differentiate. After differentiation, cells were examined for polarity markers by immunofluorescence and/or electron microscopy. For infection studies, RPTECs were infected with BKPyV, and after three days the cells were fixed and immunofluorescence staining with primary antibodies directed against BKPyV VP1 and agnoprotein was performed.

**Results:** Immunofluorescence microscopy demonstrated that adult RPTECs, immortalized RPTECs and urinary cells developed a polarized morphology with microvilli, primary cilium and apicobasal polarity. Electron microscopy of adult RPTECs confirmed the presence of microvilli. In contrast, fetal RPTECs did not polarize in culture. After polarization, adult RPTECs were still permissive for BKPyV-infection as shown by agnoprotein- and VP1-staining three days after infection.

**Conclusions:** Adult human RPTECs, immortalized RPTECs and urinary cells develop a polarized morphology on permeable supports. Polarized adult RPTECs are permissive for BKPyV infection. These cell culture models will be useful for research on BKPyV.

## Abbreviations

BKPyV	BK Polyomavirus
RPTEC	Renal proximal tubular epithelial cells
EPP	Epithelial polarity programme
ECM	Extracellular matrix
IF	Immunofluorescence
EM	Electron microscopy
ZO-1	Zona occludens-1
Na/K-ATPase	Sodium-potassium ATPase
CK	Cytokeratin
FITC	Fluorescein
P-gp	P-glycoprotein
R123	Rhodamine-123
3D	Three dimensional
MDCK	Madine-Darby Canine Kidney
LLC-PK1	Lilly Laboratories Cell-Porcine Kidney 1
Caco-2	Cancer coli-2
RPTEC/TERT1	RPTECs immortalized with telomeras reverse transcriptase 1
ciPTEC	Conditionally immortalized proximal tubular epithelial cells
2D	Two dimensional

2.5D	Two-and-a-half dimensional
SV40	Simian virus 40
REGM	Renal epithelial growth medium
FBS	Fetal bovine serum
TEM	Transmission electron microscopy
SEM	Scanning electron microscopy
DPBS	Dulbecco's phosphate buffered saline
dps	days post seeding



# Introduction

## Polarized epithelial cells

Epithelial cells are specialized cells that line the lumen of several organs and structures. For instance, the renal tubules, intestines and pulmonary bronchi all have lumens lined with specialized epithelial cells. Although these tissues and structures have different functions, the epithelium lining their lumens perform many of the same task - it acts as a barrier and controls the transport and flow of molecules and solutes across the epithelium and increases the mechanical strength of the tissue (1-6). To do this, polarization of the epithelial cells is essential.

In polarized cells, macromolecules, such as proteins and lipids, the cytoskeleton and organelles are asymmetrically distributed throughout the cell. In epithelial tissues, this asymmetry yields two distinct membrane domains, an apical and a basolateral domain. This asymmetry is called apicobasal polarity and is crucial for the function of epithelial tissues (2, 3, 5). The apical domain constitutes the top portion of the cell with the microvilli brush border and a primary cilium. It is free of cell-cell contacts and face the lumen in tubular organs (5). The basolateral domain covers the lateral and basal membrane (2, 3). The lateral membrane has several cell-cell-contacts and junctions that connect the apical and basal membrane, while the basal membrane is opposite to the apical membrane and in contact with extracellular matrix and the basement membrane (5).

The apical membrane is responsible for secretion and uptake of solutes and molecules, as well as acting as a barrier, restricting flow of solutes and hindering pathogens from crossing the monolayer. Together with tight junctions, the apical membrane makes up the paracellular barrier. Additionally, the apical membrane has microvilli and a single primary cilium. The primary cilium, together with apical microvilli, gathers important sensory information, such as flow in the renal tubules (7, 8). The lateral parts of epithelial cells in the epithelial lining is connected through junctions in the lateral domain, specifically tight and adherence junctions. These junctions are important for binding the individual cells in the epithelium together, yielding mechanical strength to the epithelium. The apical and basolateral membrane of epithelial cells are each connected with a separate compartment,

the apical lumen or the interstitial space, respectively (1-3). In the basal part of the cells, the cells are enriched in extracellular matrix (ECM) receptors, such as integrins, that anchors the cells to the extracellular matrix and basement membrane (2). Like the apical membrane, the basal and lateral membrane also have several different transporters, e.g. sodium-potassium ATPase, partaking in the flow of molecules and solutes across the cell layer.

Initiation and establishment of polarity is dependent on the epithelial polarity programme (EPP) (3). The EPP consists of several conserved protein groups; the Crumbs complex, the Par system, Scribble and Rho GTPases, that all play vital parts in regulation of polarization (3, 4). Polarization starts with symmetry breaking caused by a cue. Examples of cues that can contribute to symmetry breaking are ECM-contacts, developmental cues, cell-cell contacts and chemical cues (5). After symmetry breaking, polarity is established by asymmetric targeting and localization of proteins, lipids, macromolecules to the plasma membrane as well as reorganization of the organelles and cytoskeleton (5). Apically, the PAR-proteins, atypical protein kinase C and the Crumbs complex reside (6), while PAR-1 and the Scribble proteins are most important for establishment of the basolateral domain and are essential for excluding apical proteins from the basolateral domain (4-6).

After initiating polarization, the EPP maintains polarity through mutual exclusion between the apical and basolateral polarity proteins. This antagonism excludes apical polarity proteins from the basolateral domain and vice versa. Mutual exclusion is essential for correct localization of junctional complexes and the formation of a non-overlapping apical and basolateral domain. If this antagonism is shifted or disrupted, a specific membrane domain can expand or overlap the other domain (4, 5).

### Markers of polarity

As already mentioned, polarized epithelial cells have several known features and structures. The presence of these features can therefore be used to assess if cells are polarized.

Immunofluorescence (IF) microscopy and electron microscopy (EM) are two much used and suitable methods to assess if such features are present. IF microscopy can be used to assess protein expression and localization and if a cell has two distinct membrane domains. EM allows for the direct visualization of subcellular structures.

The primary cilium is a specialized sensory organelle present on most mammalian cells (7, 9). It is a solitary organelle or structure that protrudes from the apical membrane into the extracellular environment (2) and partakes in several different processes depending on the cell and organ (7, 9). In the kidney, the primary cilium is important for sensing of urine flow and correct renal tubular cell morphology (9, 10). Studies have also shown that polarized renal epithelial cells in different cell models develop a primary cilium (11, 12). With IF microscopy, the primary cilium can be visualized by staining cells for acetylated tubulin (12). When examined with IF, the primary cilium is visualized as a distinct stained punctum or a snaking line at the apical membrane of the cell. In the lateral view of confocal microscopy images, the primary cilium is seen as a solitary structure that protrudes from the apical membrane (12, 13). Additionally, the primary cilium can be directly visualized by EM (12).

Microvilli, finger-like protrusion of the apical membrane, is another morphological feature of polarized epithelial cells (2, 14). They are present on many polarized cell types, for instance renal proximal tubular epithelial cells and intestinal epithelial cells (15, 16). Microvilli increase the surface area of epithelial cells and are important for sensing and modulating tubular flow and reabsorption (8). To visualize microvilli, both electron microscopy and IF microscopy is suitable. EM allows one to directly visualize the individual microvilli (16), while for IF, microvillous proteins are used as markers to visualize the apical brush border (12). Ezrin and villin are two examples of proteins often used to visualize the microvilli by IF microscopy (12).

Tight junctions and adherens junctions are two structures in the lateral membrane of polarized epithelial cells (2, 17). Tight junctions are localized at the junction between the apical and the lateral membrane and act as an intercellular barrier. The barrier separates the apical and basolateral compartment and restricts paracellular transport and flow of solutes and molecules (17). To examine if cells have tight junctions, proteins in the tight junction-complex can be examined by IF microscopy and used as markers for tight junctions, allowing one to assess the presence and localization of the junctions. Zona occludens-1 (ZO-1) is a tight junction protein that is often used to assess if cells have tight junctions. Other tight junction proteins frequently used are occludins and claudins (18).

The adherens junctions are localized more basal compared to tight junctions. They attach the epithelial cells to each other and provide adherent strength to the epithelium (17). Catenin and cadherin are examples of important adherens junction-proteins, with epithelial cadherin (E-cadherin) as the most abundant. Like tight junction-proteins, proteins in the adherence junctions can be utilized to assess if cells have adherens junctions and where they are localized. Lastly, adherens junctions and adherens junction-proteins are a feature of the basolateral membrane and can therefore be used as a marker of the basolateral membrane. In addition to IF-staining, tight junctions and adherence junctions can be visualized by EM. On EM, both tight and adherens junctions appear as electron dense fusions of the lateral membrane between neighboring cells (19, 20).

Integrins are ECM-receptors localized to the basal membrane, where they facilitate cell-ECM adhesion. Because of their localization, they are markers for the basolateral membrane (1, 17).

The sodium-potassium ATPase (Na/K-ATPase) enzyme is a protein transporting sodium and potassium across the plasma membrane (12, 21). In epithelial cells with an established apicobasal polarity, Na/K-ATPase is restricted to the basolateral membrane, while in non-polarized cells it is localized in the entire plasma membrane (22, 23). This restriction of Na/K-ATPase to the basolateral membrane makes it a useful marker of apicobasal polarity and the basolateral membrane. Furthermore, Na/K-ATPase can be used to assess if cells have separate membrane domains or a symmetrical, single domain plasma membrane.

Cytokeratins (CK), a group of cytoskeletal intermediate filaments, is another group protein expressed in polarized epithelial cells. CKs are differentially expressed across different cells and tissues and can therefore be used as a marker for polarized epithelial cells (24, 25). For instance, cytokeratin-18 (CK-18) have been shown to be present in renal epithelial cells (24).

Cell shape and height are morphological characteristics that can be assessed. Polarized epithelial cells typically have a cylindrical or cuboidal shape, while unpolarized cells are more elongated. Cell height is another feature of polarization, as increased cell height is a sign of polarization (21). Both EM and IF microscopy is suitable for assessing the shape and height of cells.

## Functionality of polarized cells

In addition to morphological features and characteristics, the functionality of the cells can be assessed experimentally. Polarized epithelial cells have an important barrier function and control flow of molecules and solutes across the epithelial layer (4, 5). These functions can be assessed in vitro through different assays. Tight junctions are paramount for the epithelium's barrier function. The leak-tightness of the cell layer is therefore a way to assess the function of the tight junctions in the cell layer (12, 26, 27). This can be assessed with a permeability assay where a macromolecule coupled to fluorescein (FITC) is added to the apical compartment followed by measuring of fluorescence in the basolateral compartment. This assay has been used to assess barrier permeability in a wide range of cell lines (12, 26, 28, 29). If the cell layer functions as a barrier, the fluorescing macromolecule is restricted to the apical compartment and followingly there is only a low or no fluorescent signal in the basolateral compartment (12, 26, 28, 29).

In addition to being leak-tight, polarized epithelial cells have several transporters and influx and efflux pumps. The pumps enable the cells to absorb and secrete substrates as well as trans-epithelial transport of substrates (12, 30-33). Examining the function and presence of known transporters in the kidney or other tubular organs is therefore one way to assess if a cell layer has similar functionality as polarized epithelial layers.

P-glycoprotein (P-gp) is a known efflux pump of the renal proximal tubules and is important for renal excretion of various substrates. Followingly, P-gp is a suitable target to examine if a renal cell culture model has a proximal tubule-like functionality and polarity. The calcein accumulation assay and rhodamine-accumulation assay are two well-known assays to examine P-gp function (12, 30-32, 34). Calcein and rhodamine-123 (R-123) are fluorescent dyes that passively diffuse into cells. Both dyes are substrates of P-gp and are therefore excreted by P-gp at the apical membrane. Normally, most of the dyes are excreted by P-gp, but if P-gp is inhibited, the intracellular fluorescence increases as the dyes are retained intracellularly. The assay therefore compares intracellular with and without a P-gp inhibitor and if the intracellular fluorescence increases when P-gp is inhibited, it shows that the cells have a functional P-gp pump (30, 31, 35).

Additionally, R-123 can be used to assess transepithelial transport as it can be transported from the basolateral compartment to the apical compartment. The dye is absorbed at the basolateral membrane via organic cation transporters and pumped out by P-gp at the apical membrane. The trans-epithelial transport assay or rhodamine-transport assay can be utilized to assess trans-epithelial transport as well as the function of P-gp and organic cation transporters in epithelial cells cultured on permeable supports or in three-dimensional (3D) cell culture (12, 32, 33).

Another essential task of the proximal tubule is receptor-mediated endocytosis and fluid-phase endocytosis (36, 37). Receptor-mediated endocytosis is mediated at the apical membrane of polarized epithelial layers by cubulin and megalin. The two proteins have several known substrates, for example albumin (36). By utilizing known substrate of receptor-mediated endocytosis coupled to a fluorescent dye, the megalin/cubulin-transport system and receptor-mediated endocytosis can be assessed by using intracellular fluorescence as a marker for endocytosis (15, 36, 38, 39). Fluid-phase endocytosis can be measured in a similar way but utilizing a substrate, e.g FITC-dextran, of fluid-phase endocytosis (40, 41).

### Epithelial cells and cell lines for polarization studies

Today, a wide range of immortalized epithelial cell lines and primary epithelial cells are available from numerous commercial sources. Cell lines are often used in polarization studies and there are several well-characterized immortalized epithelial cell lines differentiate and form polarized epithelial monolayers and cysts in vitro. Madine-Darby Canine Kidney (MDCK) cells, Lilly Laboratories Cell-Porcine Kidney 1 (LLC-PK1) and Cancer coli-2 (Caco-2) cells are examples of such established cell models. MDCK are canine kidney cells, LLC-PK1 is a pig kidney cell line (42-46) and Caco-2 is a human colorectal adenocarcinoma cell line (47, 48). All three cell lines form a polarized cell layer with microvilli and intercellular junctions (21, 42-45, 47, 48). Although well-established, a major drawback is that none of them are primary human epithelial cells.

Renal proximal tubular epithelial cells (RPTECs) have been immortalized with human telomerase reverse transcriptase-1 (TERT1) and are available as the RPTEC/TERT1 cell line (15, 49). They are not nearly as well-studied in polarization studies as the previously

mentioned cell lines, but RPTEC/TERT1 have been shown to form polarized tubules in Matrigel (50). Another option is the conditionally immortalized human proximal tubule epithelial cell line (ciPTEC). The ciPTECs can be developed from renal tissue or urine, is of renal origin, has proximal tubule-like characteristics and can form polarized monolayers in vitro (31, 51, 52).

Lastly, RPTECs with finite lifespan are available from numerous commercial sources. Lonza and ScienCell are two companies that offer RPTECs. Lonza state that their RPTECs form tubules on Matrigel, can polarize under specific conditions and stain positive for pan-cytokeratin, while ScienCell have confirmed that their RPTECs express CK-18 and CK-19 (53, 54), two known markers of renal epithelial cells (55, 56). In addition to the commercially available RPTECs, RPTECs can be obtained from human material such as kidney biopsies, kidneys unsuited for grafting and from nephrectomies. Several publications have described culture of primary RPTECs from such materials (12, 57-61). Unfortunately, kidney biopsies and nephrectomies are invasive medical procedures, greatly reducing the accessibility to such materials. An easy and non-invasive alternative can therefore be to isolate exfoliated urinary cells from urine. It has previously been shown by several groups that urinary cells are culturable. Furthermore they are epithelial-like, originate from renal epithelium and express renal epithelium markers (12, 62-64). Urine can therefore be an available and practical source of primary renal tubular epithelial cells.

### Epithelial cell culture models

A wide range of cell culture models have been developed with the aim of mimicking the in vivo morphology and structure of epithelial tubular organs. The intestine, kidney and the airways are among the organs that have been modelled in multiple models of varying complexity (47, 48, 65-68). Renal cell culture models aim to imitate the in vivo function and cellular architecture of the nephron with filtration and active secretion and reabsorption of solutes. The kidney is a complex organ with several components, and the models therefore differ in complexity from simple two-dimensional (2D) cell cultures to extremely complex kidney organoids (69, 70). The simpler models often aim to model a single nephron segment, for instance the proximal tubule or the collecting duct, while the more complex models include several different cell types and model more than one segment.

The simplest models are two-dimensional cell cultures of renal epithelial cells, primary cells or a cell line, cultured on plastic or glass (43, 51, 61, 64, 71-73). 2D cell culture models lack two separate compartments, as the cells are cultured in a plastic dish or well with a single compartment.

To establish more complex and in-vivo like cell culture models, there are several available tools, for instance the permeable support. Permeable supports are cell culture well inserts with a membrane where cells can be cultured. The membrane has multiple pores of a given size, making it permeable to water and solutes. By placing the permeable supports in a cell culture well, the membrane separates the well from the compartment inside the support, yielding two compartments separated by a permeable membrane with cells seeded on one side of the membrane. Cells can be seeded on both sides of the membrane (as illustrated in illustration 1). The side where the cells are seeded is the apical compartment, while the compartment without cells is the basal compartment (Illustration 1). Typically, the apical compartment is inside the insert while the basolateral compartment is the well (74). The two separate compartments yield a two-and-a half dimensional (2.5D) cell culture model. Such models can be utilized to mimic tubular organs or blood vessels with a luminal compartment and an intercellular compartment such as the kidneys, intestines and other blood-tissue barriers (5, 21, 46, 75-77). For the kidneys, several publications have already described culture of polarized human and animal renal epithelial cells on permeable supports (39, 78-84). Compared to 2D-models, the separate compartments of a 2.5D-model provide more in vivo-like conditions and have several advantages over 2D-models. The two compartments allow for manipulation of the apical membrane and the basolateral membrane independently of each other. Furthermore, epithelial cells grown on permeable supports have been shown to differentiate into a more polarized phenotype (74). Moreover, primary human RPTECs have been shown to develop a more polarized phenotype when cultured on permeable filters (79, 84) and murine RPTECs lose their epithelial organization when not cultured on permeable filters (39).

Another use of permeable supports and 2.5D-models are transport studies of solutes, macromolecules, chemicals or drugs (21, 85) as the two separate compartments permit assessment of transepithelial transport and the barrier integrity of a monolayer. This is not possible in a 2D-model, as barrier integrity and transepithelial transport cannot be examined



without two separate compartments. The two compartments can also be utilized for studying host-pathogen interactions, for instance how a pathogen invades a monolayer, which membrane domain a pathogen can attach to and enter (86, 87) and if the release of a pathogen is polarized and which membrane domain it exits.

Lastly, 3D cell culture models and organoid models is the most complex cell culture models. Polarized 3D cultures of a renal epithelial cell line have already been described. For instance, epithelial cells are cultured between two layers of Matrigel form 3D tubules with polarized epithelial cells (50). Compared to a 2.5D-model, the tubular phenotype is more in vivo-like with stronger expression of polarity markers. A drawback of 3D-models is that the apical membrane is not as accessible for manipulation as in a 2.5D-model. Other 3D-models have been established by utilizing organ-on-a-chip technology and microfluidics (67, 88). Lastly, several complex kidney organoid models have recently been described (89). Organoid models yield superior complexity and morphology, but as for other 3D-models, only one of the membrane domains are accessible to experimental manipulation.

Numerous models of polarized epithelial cell culture models are described in the scientific literature as these models are relevant and offers many opportunities. This is showcased by their use in a wide range of fields, such as toxicology, pharmacology, hereditary diseases, infectious disease modelling, organ development and oncology (12, 48, 50, 74, 86, 89, 90).

Today, there is no established and universally used model for polarized RPTECs, but rather multiple different models used in a range of different fields. As there is no consensus model, the researcher must rather choose a model suited for their research question and field.

### **BK Polyomavirus research lacks a polarized cell model**

BK Polyomavirus (BKPyV) is a small non-enveloped DNA virus in the family of Polyomaviridae. Most people are infected at a young age followed by establishment of a lifelong persistent infection in the kidney tubular epithelial cells and bladder urothelium. Immunocompetent individuals will periodically shed BKPyV in the urine, but this does not affect the kidney function or cause symptoms. In immunocompromised hosts, such as kidney transplant patients and allogeneic hematopoietic stem cell recipients, BKPyV can undergo high-level replication and cause severe disease. In kidney transplant recipients, BKPyV cause

polyomavirus-associated nephropathy, while stem cell recipients can develop polyomavirus-associated hemorrhagic cystitis (91).

The tubular epithelial cells of the kidney are highly differentiated and polarized epithelial cells. Although the natural host cell of BKPyV are polarized tubular epithelial cells, most of the previous work on BKPyV's replication cycle has not been performed in primary polarized RPTEC, but with non-polarized RPTECs and simian kidney cell lines.

Polarized epithelial cells differ significantly from non-polarized cells and the viral replication cycle may therefore be different in polarized epithelial cells compared to non-polarized cells. Additionally, several viruses have already been shown to have a polarized entry and release in polarized epithelial cells and cell lines (86, 90, 92-101). This may also be the case for BKPyV, but a polarized cell culture model is necessary to examine this issue. To examine this further we wish to establish a polarized 2.5D-model of RPTECs on permeable supports.

The proposed cell culture model of polarized RPTECs can be used to examine several important issues of BKPyV's replication cycle such as determining if entry and release of BKPyV is polarized. Simian virus 40 (SV40), a simian polyomavirus, has previously been shown to have a polarized replication cycle (86, 90), but this has not been investigated in BKPyV. Which membrane domain the virus enters and exits from is relevant for several unanswered issues of BKPyV infection and pathogenicity. We currently do not know whether the virus reaches the renal tubular epithelial cells via blood or the glomerular filtrate. If BKPyV infects the RPTECs via glomerular filtrate, it must be able to bind and enter the host cell from the apical membrane, while infection from the blood means that it must be able to enter the host cells through the basolateral membrane.

Another issue is the release of BKPyV. BKPyV has been reported to exit the host cell through lysis (102) and in immunocompromised patients, BKPyV may cause a lytic infection. The lysis leads to a massive release of infectious virus particles and subsequent viremia (91). However, it is still unclear if BKPyV can exit the host through a non-lytic mechanism. Healthy individuals can shed BKPyV asymptotically and the lack of symptoms, low viral titer and lack of viremia can be the result of non-lytic spread of BKPyV. For SV40, one publication has described polarized non-lytic release in a polarized epithelial cell line (90), while different forms of non-lytic release have recently been described for BKPyV and JC Polyomavirus (103-

105). More research is needed on this issue and a polarized cell model can be a useful tool for this area of BKPyV research. Studying the viral replication cycle in a polarized cell model can contribute to answering these questions, as the model permits examination and manipulation of the apical and basolateral membrane separately. This will allow investigation of which membrane domain the virus enters and exits the cells from, which again can contribute to new hypotheses regarding BKPyV infection and spread in vivo.

Today, the consensus model used for in vitro studies of BKPyV are unpolarized RPTECs. Although unpolarized RPTECs have contributed greatly to our understanding of the replication cycle of BKPyV, they also have drawbacks. As BKPyV infects polarized epithelial cells in the reno-urinary tract, a polarized cell culture model would be a more relevant model for modelling BKPyV infection. Furthermore, non-polarized cells are vastly different from polarized cells and it is therefore not given that the replication cycle is equal in polarized cells. Therefore, a polarized RPTEC model would be a useful and relevant tool for future research on BKPyV. Recently, BKPyV-infection was for the first time modelled in a kidney organoid (12), showcasing the increasing interest for more complex cell culture models in studies of BKPyV.

By establishing a 2.5D-model of RPTECs, we wish to expand our repertoire of cell culture models to further investigate the replication cycle of BKPyV.

## Aim

The aim of this study was to establish a polarized 2.5D-cell culture model of human RPTECs.

The aim was further divided into the following objectives:

1. Examine the morphology of RPTECs and RPTEC/TERT1s cultured on permeable supports by electron microscopy and immunofluorescence imaging and investigate if known markers of epithelial cell polarity are present.
2. Isolate urinary cells from urine and compare them morphologically to commercially available RPTECs.
3. Examine if polarized RPTECs are permissive to BKPyV infection.

## Material and methods

### Materials and cells

Primary human RPTECs were bought from Lonza (CC-2553) and ScienCell (#4100). RPTECs were cultured in renal epithelial growth medium (REGM; Lonza) containing 0.5% fetal bovine serum (FBS). RPTECs from both Lonza and ScienCell were used at passage 3. RPTEC/TERT1s (ATCC-CRL-4031) were cultured in REGM containing 2% FBS and used at passage 22-28. All cells were cultured in a humidified 5% CO<sub>2</sub> incubator at 37°C.

Transwell polyester permeable supports with pore size 0,4 µm were bought from Corning (#3470). Recombinant human collagen type 1 was bought from Sigma-Aldrich (C7624, Sigma-Aldrich). Labtek confocal chamber slides were from Thermo Fisher. Mowiol mounting medium was kindly supplied by the Advanced microscopy core facility at UiT. Human fibronectin was supplied by Peter McCourt at the Vascular Biology research group at UiT.

### Virus

Infectious supernatants were produced by infecting Vero cells (ATCC CRL-1586) with BKPyV (Dunlop-strain) follow by harvesting of medium once per week. The supernatant was harvested three weeks post infection and clarified by centrifugation. The viral load was quantified by BKPyV-real time PCR (106).

### Isolation of cells from urine

The protocol for isolation of renal cells was adapted from Zhou et al (63). Urine was donated by an anonymous healthy male donor. Urine was collected in a sterile container and transferred to sterile 50-ml tubes. Cells were pelleted and washed in REGM, pelleted again and finally resuspended in 1 ml REGM with 10% FBS and seeded into a single well of a 12-well plate. The first 3 days post seeding, fresh REGM with 10% FBS was added each day. At 4 days post seeding, 3 ml medium was aspirated and 1 ml fresh REGM with 0,5% FBS was added. From here on, half of the medium was changed every other day. When cells reached 80-90% confluency the culture was split 1:4. At passage 3 the cells were cryopreserved.

### Collagen coating of permeable supports

Permeable supports were coated with recombinant human collagen type 1 (Sigma C7624). Collagen was added to the side that the cells would adhere to at a density of 23 µg/cm<sup>2</sup>. The

supports were incubated with collagen for two hours at 37°C. After incubation, collagen was removed, and the supports were air-dried under a tissue hood for 30 minutes. Media was then added to the insert and the well and incubated for one to three hours at 37°C before cells were seeded. To coat the bottom surface of the insert, the inserts were inverted to allow the collagen to attach.

### Polarization

Cells were seeded onto 6.5 mm Transwell polyester permeable supports with a pore size of 0.4  $\mu\text{m}$ . Permeable supports were coated with collagen, followed by seeding of cells at a density of 37 500 cells per  $\text{cm}^2$ . After seeding, cells were allowed to polarize for three to 17 days. During differentiation, medium was changed three times per week.

RPTECs and RPTEC/TERT1s were also seeded on the underside of the permeable supports. Collagen coating and cell seeding was done as described, except that the underside was coated, instead of the insert's inside. To allow seeding of cells on the underside, the inserts were inverted, and cells were allowed to attach to the underside for two to four hours. After cells had adhered to the underside of the insert, the insert was turned back and transferred to a 24-well plate.

### Culture of cells in chamber slides

Chamber slides (Sigma, Nunc Lab-Tek II) with a growth area of 0.8  $\text{cm}^2$  were coated with fibronectin by incubating the chamber slide wells with fibronectin for 5 minutes at room temperature followed by two washes with Dulbecco's phosphate buffered saline (DPBS). After coating, RPTECs were seeded at density of 37 500 cells per  $\text{cm}^2$ .

For polarization in chamber slides, RPTECs were seeded into coated chamber slides and cultured up to ten days. Medium was changed three times per week.

### Transmission and scanning electron microscopy

The transmission electron microscopy (TEM) protocol was adapted from Cocchiaro et al and Pokrovskaya et al (107, 108). Cells grown on permeable supports were first fixed in 2.5% glutaraldehyde in PHEM-buffer (60 mM PIPES, 25 mM HEPES, 10 mM EGTA, 4 mM  $\text{MgSO}_4 \cdot 7\text{H}_2\text{O}$ ) for at least 24 hours. The cells were then fixed again for 14 min in a fixative containing 4% formaldehyde, 0.5% glutaraldehyde, and 0.05% malachite green in PHEM

buffer (60 mM PIPES, 25 mM HEPES, 10 mM EGTA, 4 mM MgSO<sub>4</sub>·7H<sub>2</sub>O) (2 min vacuum on-off-on-off-on-off-on, 100 W) and washed two times with PHEM buffer. All processing was done in a Ted Pella microwave processor with a temperature control unit. Post-fixation was done with 1 % Osmium tetroxide, 1 % K<sub>3</sub>Fe(CN)<sub>6</sub> in 0.1 M cacodylic acid buffer. The cells were post-stained with 1% tannic acid and 1% uranyl acetate. Samples were then dehydrated in increasing ethanol series (30-60-96-100%) and embedded in an Epon equivalent (Agar). Ultrathin sections (70 nanometers) were cut using a diamond knife (Diatome) on a Leica UC 7 ultramicrotome and picked up on formvar-coated copper grids. Sections were imaged using a Hitachi HT7800 transmission electron microscopy with a Xarosa camera (EMSIS GmbH).

Specimens for Scanning electron microscopy (SEM) were cut out of the same membranes as the TEM-specimens during the dehydration process, and dried in a Leica EMCPD 300 Critical point dryer, followed by mounting and coating with gold palladium. Specimens were imaged in a Zeiss Sigma scanning electron microscope.

#### Immunofluorescence microscopy

Cells were fixed with ice-cold methanol for ten minutes. After fixation, cells were washed twice in DPBS. Before immunostaining, cells were blocked in DPBS with 5% goat serum. Primary and secondary antibodies were diluted in DPBS with 1% goat serum. Primary staining was performed for one hour at room temperature, followed by four washes with DPBS. Secondary staining was performed for one hour at room temperature followed by four washes with DPBS. After immunofluorescence staining, nuclei were stained with DRAQ5 for ten minutes at room temperature. The primary antibodies used were rabbit polyclonal anti-ZO-1 (1:100, 61-7300, Invitrogen), mouse monoclonal CK-18 (1:100, DC-10, Santa Cruz Biotechnology) mouse monoclonal anti-acetylated tubulin (1:100, sc-23950, Santa Cruz Biotechnology), rabbit monoclonal sodium-potassium ATPase (1:500, ab76020, Abcam), mouse anti-VP1 (1:500, 4942, Virostat) and polyclonal anti-agnoprotein rabbit serum (1:1000 (109, 110)). Nuclei were stained with DRAQ5 (1:1000, Biostatus). The secondary antibodies were anti-mouse and anti-rabbit conjugated with Alexa Fluor 488 or Alexa Fluor 568 (1:500, Molecular probes).

Membranes of permeable supports were cut out and mounted on glass slides on a drop of mowiol. Cells stained for polarity markers were imaged with a 40x objective on a ZEISS LSM800 confocal microscope with the Zen blue imaging software. Infected RPTECs were imaged on a widefield fluorescent microscope. All images were processed with ImageJ.

### BKPyV-infections

Polarized RPTECs were infected using supernatant from BKPyV-infected Vero cells. For infection, 100  $\mu$ l infectious supernatant diluted 1:2 with REGM was added to the apical compartment. Infection was performed for 2 hours at 37°C, before cells were washed twice with DPBS and fresh REGM was added. Three days post infection (dpi), cells were fixed and stained for BKPyV agnoprotein and VP1.

## Results

### RPTECs from different commercial sources exhibit different ultrastructural morphology

First, we investigated the ultrastructural morphology of RPTECs from two different sources, adult-derived and fetal-derived RPTECs. As microvilli is a known marker of polarized epithelial cells, we utilized SEM to investigate if the RPTECs had microvilli. Fetal and adult RPTECs were seeded on collagen-coated permeable supports and cultured for three to 17 days. We expected polarization to be initiated after cells became confluent as cell-cell contact is an important polarization cue (5, 6). Around three days post seeding (dps) cells became confluent, therefore three dps was used as the control time point. SEM showed that adult-derived RPTECs had microvilli at three dps before polarization (Fig. 1A), while fetal-derived RPTECs did not have microvilli (Fig. 2A). At seven dps adult-derived RPTECs had more microvilli on their apical surface compared to three dps (Fig. 1B). This increase in microvilli was still present ten, 14 and 17 dps (Fig. 1B, C and E). Unlike adult-derived RPTECs, fetal-derived RPTECs did not develop microvilli, even when cultured up to 20 days (Fig. 2B and C).

Next, we examined both types of RPTECs with transmission electron microscopy (TEM). As expected, microvilli were not present on fetal-derived RPTECs with TEM (Fig. 3A), while microvilli were present on adult-derived RPTECs (Fig. 3B). The adult-derived RPTECs formed a cell layer resembling a monolayer with a thickness of one to two cells (Fig. 3B). In contrast,

the fetal-derived RPTECs formed a thicker cell layer consisting of five to eight piled cells (Fig. 3A).

From this we concluded that the fetal-derived RPTECs examined did not polarize on permeable supports, while adult-derived RPTECs undergo changes similar to polarization. Therefore, we decided to examine adult-derived RPTECs further with IF microscopy.

### Differentiate leads to increased expression of the tight junction protein ZO-1

First, we investigated the expression of the tight junction protein ZO-1 in RPTECs by immunofluorescence microscopy. RPTECs were fixed at three dps, stained for ZO-1 and imaged. Imaging demonstrated that RPTECs express ZO-1 before polarization (Fig. 4A). The expression is quite heterogenous and varies between cells. Some cells show a distinct ZO-1 expression at the border of the cell, while a large proportion of cells do not show this pattern (Fig. 4A). Next, we investigated ZO-1 expression in cells allowed to polarize for ten and 14 days. Imaging demonstrated that RPTECs had strong expression of ZO-1 at both 10 and 14 days of culture (4B and C). Compared to the control, ZO-1 expression was stronger with a more distinct expression at the lateral membrane after differentiation (Fig. 4B and C).

Lastly, we investigated if ZO-1 was localized to distinct puncta in the subapical region of the cells. The lateral view of RPTECs confirmed that ZO-1 is localized subapically in RPTECs before polarization (Fig. 5A). After culture for ten (Fig. 5B) or 14 days (Fig. 5C), RPTECs had a similar distribution of ZO-1 in several distinct subapical puncta. Similar to EM, the lateral view showed that the thickness of the cell layer increased after differentiation and consisted of one to three cells (Fig. 5B and C). RPTECs cultured for three days was organized in a nearly confluent monolayer (Fig. 5A).

### Differentiation leads to apical-basolateral polarity

After confirming the presence of tight junctions, we wanted to examine if RPTECs have apical and basolateral domains. Therefore, we stained RPTECs with an antibody against Na/K-ATPase. RPTECs that had not undergone differentiation (three dps) exhibited strongest staining along the cells' borders (Fig. 6A), but there was also a diffuse staining throughout the cells (Fig. 6A). In RPTECs cultured on permeable supports for eight, ten and 14 days, Na/K-ATPase was redistributed to the lateral membrane (Fig 6B, C and D). The redistribution of Na/K-ATPase was present as early as eight dps (Fig. 6B), although not as evident as for the



later timepoints (Fig. 6C and D). Ten and 14 dps, RPTECs displayed strong expression of Na/K-ATPase along the cell borders. This further supports that RPTECs polarize on permeable supports.

Next, we examined the lateral view to investigate if the apical or basolateral membrane had Na/K-ATPase. The unpolarized control RPTECs had staining of the entire plasma membrane (Fig. 7A), while in RPTECs cultured for eight, ten and 14 dps (Fig. 7B, C and D), Na/K-ATPase was confined to the basolateral membrane. Although the redistribution was clearer at ten and 14 dps (Fig. 7B and C), the redistribution of Na/K-ATPase to the basolateral membrane was visible at eight dps. The lack of Na/K-ATPase in the apical membrane confirms that RPTECs developed two separate and distinct membrane domains. The presence of two distinct and separate membrane domains is a hallmark of apicobasal polarity, and thus supporting that RPTECs can polarize on permeable supports from eight days of culture.

Lastly, we examined the cell height and shape in the lateral view, as increased cell height and a cuboidal or cylindrical shape are two known markers of polarity (21). We have previously seen that non-polarized RPTECs cultured on plastic have a flat and elongated shape (results not shown). The Na/K-ATPase-antibody is suitable to examine cell shape as it stains parts of the plasma membrane. Before differentiation, the RPTECs were flat and elongated (Fig. 6A and 7A), similar to RPTECs seeded on plastic. Eight, ten and 14 dps, the cell shape was more cuboidal, less elongated and the height of the cells had increased (Fig. 6B-D and 7B-D). Similarly to the ZO-1 staining, we noticed that the RPTECs do not form a strict monolayer, but rather a cell layer that consists of one to three cells (Fig. 7B, C and D). Summarizing, IF microscopy confirmed that adult RPTECs develop two separate membrane domains and exhibit apicobasal polarity from eight dps.

### **RPTECs develop primary cilia**

We next examined if RPTECs developed a primary cilium. Before differentiation, RPTECs did not have a distinct primary cilium, but instead exhibited a diffuse cytoskeletal staining of acetylated tubulin (Fig. 8A). When cells were allowed to differentiate for eight and ten days, a large proportion of cells exhibited a distinct punctate or snaking staining at the apical membrane (Fig. 8B and C). Additionally, the diffuse cytoskeletal staining was reduced after differentiation (Fig. 8B and C). The lateral view confirmed that the punctate and snake-like

lines are in fact primary cilia, as they extend from the apical membrane and out into the apical compartment (Fig. 9B and C). In the unpolarized control (Fig. 9A), we did not see any punctate staining, only the diffuse cytoskeletal staining previously described. This was further supported by our previous SEM-images, as structures similar primary cilia was present on more cells after polarization (seven dps) (Fig. 10B) compared to the non-polarized control (Fig. 10A).

### **RPTECs seeded upside-down develop the same morphology**

For infection studies in permeable supports, it can be useful to seed the cells on the underside of the support as it allows one to invert the support and infect the apical and basolateral membrane with the same volume of virus. We therefore examined if RPTECs developed the same morphology when seeded and cultured upside-down on permeable supports. RPTECs were allowed to attach to inverted filters, before they were put into 24-well plates. This way, the cells grow on the underside of the insert instead of inside the filter. The cells attached to the underside and by ten days of culture they developed a polarized morphology with apicobasal polarity and a primary cilium (Fig. 11A and B). Like cells grown inside the support, the part of the cell positioned against the permeable filter developed into the basolateral membrane, while the domain that bordered to the medium developed into the apical membrane (Fig. 11C). This confirms that RPTECs polarize on permeable supports, regardless of which side the cells are seeded.

### **RPTEC/TERT1 polarize on permeable supports**

After examining polarization of RPTECs, we investigated if the immortalized cell line RPTEC/TERT1, can polarize on permeable supports. Like RPTECs, RPTEC/TERT1s were cultured on permeable supports for three or ten dps followed by assessment of the expression of Na/K-ATPase and acetylated tubulin by IF microscopy. At three days of culture, RPTEC/TERT1s Na/K-ATPase was diffusely distributed throughout the whole plasma membrane (Fig 12A). Surprisingly, acetylated tubulin had a punctate distribution at baseline (Fig. 12B) similar to polarized RPTECs (Fig. 9B and C). After ten days of culture, the distribution of Na/K-ATPase was stronger in the lateral membrane after differentiation (Fig. 12C), but not as clearly as for RPTECs (Fig 6C). Acetylated tubulin retained its punctate staining pattern after polarization (Fig. 12D).

We also investigated RPTEC/TERT1s in the lateral view, and unlike RPTECs, RPTEC/TERT1s did not increase in height (Fig 13A and B). The lateral view confirmed that RPTEC/TERT1s have primary cilia that protrudes from the cell at three dps and ten dps (Fig. 13C and D).

RPTEC/TERT1s undergo a change in morphology when differentiated for ten days, but the polarity is not as clear as for RPTECs (Fig. 8, 9 and 11).

### Permeable supports are not necessary for polarization of RPTECs

After confirming that RPTECs and RPTEC/TERT1s could differentiate on permeable supports, we wanted to examine if the supports were requisite for polarization. To examine this, we cultured RPTECs in chamber slides for three and ten days followed by IF microscopy. Prior to differentiation, RPTECs had diffuse staining of both Na/K-ATPase (Fig. 14A and 15A) and acetylated tubulin (Fig. 14B and 15B) Surprisingly, RPTECs differentiated in chamber slides developed a polarized morphology similar to RPTECs. RPTECs allowed to differentiate in chamber slides displayed two distinct membrane domains (Fig. 14C and 15C), a primary cilium extending out from the apical membrane (Fig. 14D and Fig. 15D) and tight junctions with ZO-1 (Fig. 16). The cells also increased in height, as evidenced by a taller Z-stack, and developed a more cuboidal shape (Fig 14C and D). Taken together, this points towards that the two separate medium compartments are not necessary for polarization.

### Cells isolated from urine are similar to commercial RPTECs

After confirming that commercial RPTECs can polarize in culture we decided to compare them to renal epithelial cells from another source. Exfoliated urinary cells have previously been shown to originate from renal epithelium (62, 63). Followingly, we decided to isolate and compare urinary cells to commercially available RPTECs. Urinary cells were isolated from the urine of an anonymous healthy male donor. After isolation by centrifugation, the cells were seeded in plastic wells in REGM and passaged. As previously shown (63), the urinary cells could be passaged on plastic. Urinary cells had an elongated and oval shape and grew in a cobblestone-like pattern (Fig. 17A) similar to RPTECs (Fig. 17B).

Next, we investigated if the urinary cells expressed CK-18. In a culture of urinary cells, the majority of urinary cells expressed CK-18 (Fig. 17C), confirming that they are epithelial cells. The commercial RPTECs from Lonza express CK-18 and were used as a positive control (Fig. 17D).

## Urinary cells polarize on permeable supports inserts

After confirming that urinary cells are culturable and express CK-18, we wanted to assess if they polarize on permeable supports. Urinary cells were seeded on collagen-coated permeable supports and allowed to differentiate for three or 14 days. After differentiation, cells were fixed and stained for the polarity markers Na/K-ATPase, ZO-1 and acetylated tubulin. Like RPTECs, urinary cells were non-polarized after three days of differentiation with a flat and elongated cell shape without basolateral Na/K-ATPase (Fig. 18A and 19A) or primary cilium (Fig. 18C and 19C). After 14 days of differentiation urinary cells exhibited a more polarized morphology. Na/K-ATPase was restricted to the basolateral membrane (Fig. 18B and 19B) and a large proportion of the cells displayed a primary cilium (Fig. 18D and 19D). Next, we assessed ZO-1 before and after differentiation. ZO-1 were present before polarization (Fig. 18E and 19E) but showed stronger staining at 14 dps (Fig. 18F and 19F). Additionally, ZO-1 was more subapically located after differentiation (Fig. 19F), while three dps ZO-1 was located more laterally (Fig. 19E). Lastly, the cell's height increased, and they developed a more cuboidal shape (Fig. 19B and 19F).

## Polarized RPTECs are permissive to BK Polyomavirus infection

After confirming that renal epithelial cells of different origin polarize on permeable supports, we investigated if adult polarized RPTECs are permissive to BKPyV infection. RPTECs were cultured for eight and 14 days followed by infection with BKPyV at the apical side. Three days post infection, cells were fixed and stained for BKPyV agnoprotein and BKPyV VP1. Cells cultured for 14 days stained positive for VP1 and agnoprotein after infection (Fig. 20A), confirming that they are permissive for and support BKPyV replication. Mock infected cells did not stain positive for either agnoprotein or VP1 (Fig. 20B).

## Discussion

In this study we have established and characterized polarized epithelial cell models of adult RPTECs, RPTEC/TERT1s and urinary cells. All three cell types developed a polarized morphology with several known markers of apicobasal polarity. Furthermore, adult RPTECs retained their susceptibility to BKPyV, an important requisite for the cell culture model to be a viable model for studying BKPyV.

In our study, fetal RPTECs did not polarize despite differentiation on permeable supports. The other renal epithelial cells were of adult origin and this may be the reason that they polarized. To our knowledge, attempts at polarizing fetal-derived RPTECs have not been described before.

Adult RPTECs did not only polarize on permeable supports but polarized when cultured in chamber slides. This points toward that the two separate membrane compartments are not necessary for polarization and there may have been other cues that were responsible for initiating polarization. Cell-cell contacts and ECM-interactions are two known drivers of apicobasal polarity and these interactions can initiate polarization in vitro (5, 111). In our cell culture, cells were seeded on a collagen-matrix, were confluent and developed cell-cell contacts. These stimuli may have been enough to drive polarization, making the permeable supports dispensable for polarization.

The existing literature is divided on the role of permeable supports for polarization. Two studies of human RPTECs and one study of mouse RPTECs have showed that permeable supports lead to a more polarized morphology (39, 79, 84). In contrast, it has also been reported that RPTEC, RPTEC/TERT1 and ciPTECs can display polarized features in 2D-culture (15, 51). Although permeable supports may not be necessary for polarization, they are still a useful tool as they make the basolateral membrane accessible. In a well or chamber slide, only the apical domain is accessible for manipulation, while permeable supports allow us to manipulate the two membrane domains separately from each other. This makes permeable supports useful for modeling infectious diseases as it allows us to examine which membrane domain a pathogen binds to, invades or is released from. For BKPyV, this model will allow us to examine which membrane domains BKPyV can enter and exit from. This has already been examined for a wide range of viruses, including a simian polyomavirus (86, 90, 96, 97, 100, 112), but not for BKPyV.

Like adult RPTECs, urinary cells developed a polarized morphology similar to the renal epithelial cells. This is in line with previously published reports. Two publications have shown that urinary cells are of renal origin (51, 113), while a third publication showed that urinary cells display a polarized morphology, although it is less prominent compared to epithelial cells from kidney tissue (31). In our study, a large proportion of the urinary cells stained

positive for CK-18, a marker of renal epithelial cells. However, the urinary cells may originate from other parts of the reno-urinary tract as several cell types in the reno-urinary tract express CK-18 (24). One study, found that urinary cells could originate from both the kidney and the bladder (12). The CK-18 positive and CK-18 negative cells may therefore represent two different cell types from the reno-urinary tract. This is supported by three papers that have described that cell populations isolated from urine can contain a mix of cell types (12, 64, 114). Nevertheless, urine is an accessible and useful source to isolate reno-urinary epithelial cells with the capacity to polarize. If confirmed that they are susceptible to BKPyV, polarized urinary cells can be a viable and useful cell culture model for BKPyV.

Lastly, we confirmed that polarized RPTECs retain their susceptibility for BKPyV infection. This confirms the potential and usefulness of polarized RPTECs as a cell culture model for BKPyV. Much research has been done on BKPyV since its discovery and this has substantially increased our understanding of the replication cycle of BKPyV. However, our current knowledge of BKPyV is almost exclusively from studies using non-polarized epithelial cell culture models. This is a large drawback as BKPyV infects polarized epithelial cells in vivo. Unlike non-polarized epithelial cells, polarized epithelial cells have asymmetrical distribution and transport of macromolecules and organelles. Since viruses exploit host molecules and organelles for entry, replication and exit, asymmetrical distribution and expression of these factors may affect the replication cycle of a virus. Furthermore, the transport of cargo is asymmetrical in polarized epithelial cells (5, 6). BKPyV, and other viruses, is transported within the host cell by cellular proteins (115), and it is therefore possible that the intracellular transport of viruses differ between polarized and non-polarized epithelial cells. This possibility is further supported by several studies that have shown how polarization can affect the replication cycle of a range of viruses (86, 116, 117). Because of this, a polarized renal cell culture model is a powerful and needed tool to study the replication cycle of BKPyV in a more relevant setting.

Microvilli, primary cilium, strict basolateral distribution of Na/K-ATPase and subapical ZO-1 are all well-documented markers for polarity (12). Our use of validated polarity markers is a strength of our study. Moreover, our results are in line with the existing literature (31, 50, 51, 60, 80, 118-120). Another strength of the study is that we have investigated three different types of renal epithelial cells, displaying that the ability to polarize may be a

general trait of adult renal epithelial cells. Importantly, we also confirmed that adult RPTECs are susceptible to BKPyV infection after polarization. This is in line with a recent paper that modelled BKPyV infection in a kidney organoid model (12).

A weakness of our adult RPTEC-model is that the cells do not develop a strict monolayer but rather a cell layer consisting of one to two cells (Fig. 7D). However, it can be challenging to assess the monolayer and cell layer thickness as cells that only overlap slightly can be visualized as lying on top of each other. ZO-1 is also challenging to visualize as it is subapically localized, and the permeable supports are not level when mounted on glass slides. This makes it difficult to keep ZO-1 in focus throughout the entire field of view and contributes to some of the heterogeneity in the ZO-1 images. Another drawback is that RPTEC/TERT1 and urinary cells were only examined with IF microscopy and not EM. The unconfirmed origin of the urinary cells is another a weakness of our study. Despite this, we still believe the urinary cells is a relevant cell culture model for reno-urinary epithelial cells. The biggest drawback of this study is that we have not investigated the functionality of the cell model. The functionality of both transporters and the epithelial barrier can be assessed in vitro through several described assays (12, 30). The barrier function of polarized renal epithelial cells is especially relevant to assess, as it is important to know if BKPyV crosses the monolayer before one examines which membrane domain BKPyV enters and exits from. Additionally, functional studies would allow us to assess if there is a functional difference between Further research on the functionality of this cell culture model is therefore warranted. RPTECs polarized in chamber slides or permeable supports, despite their similar morphology.

Lastly, we have not confirmed that polarized urinary cells and RPTEC/TERT1 are susceptible to BKPyV infection and this must be done before polarized RPTEC/TERT1s and urinary cells can be used to study BKPyV infection.

## Conclusions

In this study we have established and characterized a polarized epithelial cell models of adult RPTECs, RPTEC/TERT1s and urinary cells. All three cell types developed a polarized morphology similar to previous descriptions of polarized renal epithelial cell cultures.

However, not all RPTECs were able to polarize, as the fetal RPTECs did not polarize. Polarized adult RPTECs retained their susceptibility to BKPyV, confirming that they are a viable polarized cell culture model for BKPyV. The functionality of polarized RPTECs should be further assessed to confirm they also display a proximal tubule-like functionality. Based on our results, polarized RPTECs is a useful model for modelling BKPyV's replication cycle in a more relevant cell culture model.



## References

1. Lee JL, Streuli CH. Integrins and epithelial cell polarity. *J Cell Sci.* 2014;127(15):3217.
2. St Johnston D, Ahringer J. Cell Polarity in Eggs and Epithelia: Parallels and Diversity. *Cell.* 2010;141(5):757-74.
3. Rodriguez-Boulan E, Macara IG. Organization and execution of the epithelial polarity programme. *Nat Rev Mol Cell Biol.* 2014;15(4):225-42.
4. Roignot J, Peng X, Mostov K. Polarity in mammalian epithelial morphogenesis. *Cold Spring Harb Perspect Biol.* 2013;5(2):a013789.
5. Pickett MA, Nature VF, Feldman JL. A Polarizing Issue: Diversity in the Mechanisms Underlying Apico-Basolateral Polarization In Vivo. *Annu Rev Cell Dev Biol.* 2019;35:285-308.
6. Riga A, Castiglioni VG, Boxem M. New insights into apical-basal polarization in epithelia. *Curr Opin Cell Biol.* 2020;62:1-8.
7. Singla V, Reiter JF. The Primary Cilium as the Cell's Antenna: Signaling at a Sensory Organelle. *Science.* 2006;313(5787):629.
8. Du Z, Duan Y, Yan Q, Weinstein AM, Weinbaum S, Wang T. Mechanosensory function of microvilli of the kidney proximal tubule. *Proc Natl Acad Sci U S A.* 2004;101(35):13068-73.
9. Praetorius HA, Spring KR. Bending the MDCK cell primary cilium increases intracellular calcium. *J Membr Biol.* 2001;184(1):71-9.
10. Hanaoka K, Qian F, Boletta A, Bhunia AK, Piontek K, Tsiokas L, et al. Co-assembly of polycystin-1 and -2 produces unique cation-permeable currents. *Nature.* 2000;408(6815):990-4.
11. Sfakianos J, Togawa A, Maday S, Hull M, Pypaert M, Cantley L, et al. Par3 functions in the biogenesis of the primary cilium in polarized epithelial cells. *J Cell Biol.* 2007;179(6):1133-40.
12. Schutgens F, Rookmaaker MB, Margaritis T, Rios A, Ammerlaan C, Jansen J, et al. Tubuloids derived from human adult kidney and urine for personalized disease modeling. *Nat Biotechnol.* 2019;37(3):303-13.
13. Larre I, Castillo A, Flores-Maldonado C, Contreras RG, Galvan I, Muñoz-Estrada J, et al. Ouabain modulates ciliogenesis in epithelial cells. *Proc Natl Acad Sci U S A.* 2011;108(51):20591-6.
14. Pelaseyed T, Bretscher A. Regulation of actin-based apical structures on epithelial cells. *J Cell Sci.* 2018;131(20):jcs221853.

15. Wieser M, Stadler G, Jennings P, Streubel B, Pfaller W, Ambros P, et al. hTERT alone immortalizes epithelial cells of renal proximal tubules without changing their functional characteristics. *Am J Physiol Renal Physiol*. 2008;295(5):1365-75.
16. Mukherjee TM, Williams AW. A comparative study of the ultrastructure of microvilli in the epithelium of small and large intestine of mice. *J Cell Biol*. 1967;34(2):447-61.
17. Giepmans BNG, van Ijzendoorn SCD. Epithelial cell–cell junctions and plasma membrane domains. *Biochimica et Biophysica Acta (BBA) - Biomembranes*. 2009;1788(4):820-31.
18. Kim S, Kim G-H. Roles of claudin-2, ZO-1 and occludin in leaky HK-2 cells. *PLoS One*. 2017;12(12):e0189221.
19. Cichon C, Sabharwal H, Rüter C, Schmidt MA. MicroRNAs regulate tight junction proteins and modulate epithelial/endothelial barrier functions. *Tissue barriers*. 2014;2(4):e944446-e.
20. Hudspeth AJ. Establishment of tight junctions between epithelial cells. *Proc Natl Acad Sci U S A*. 1975;72(7):2711-13.
21. Vinaiphath A, Charngkaew K, Thongboonkerd V. More complete polarization of renal tubular epithelial cells by artificial urine. *Cell Death Discov*. 2018;4(1):47.
22. Katz AI. Renal Na-K-ATPase: its role in tubular sodium and potassium transport. *Am J Physiol Renal Physiol*. 1982;242(3):207-19.
23. Shoshani L, Contreras RG, Roldán ML, Moreno J, Lázaro A, Balda MS, et al. The polarized expression of Na<sup>+</sup>,K<sup>+</sup>-ATPase in epithelia depends on the association between beta-subunits located in neighboring cells. *Mol Biol Cell*. 2005;16(3):1071-81.
24. Achtstätter T, Moll R, Moore B, Franke WW. Cytokeratin polypeptide patterns of different epithelia of the human male urogenital tract: immunofluorescence and gel electrophoretic studies. *J Histochem Cytochem*. 1985;33(5):415-26.
25. Franke WW, Schiller DL, Moll R, Winter S, Schmid E, Engelbrecht I, et al. Diversity of cytokeratins: Differentiation specific expression of cytokeratin polypeptides in epithelial cells and tissues. *J Mol Biol*. 1981;153(4):933-59.
26. Petit L, Gibert M, Gourch A, Bens M, Vandewalle A, Popoff MR. *Clostridium perfringens* epsilon toxin rapidly decreases membrane barrier permeability of polarized MDCK cells. *Cell Microbiol*. 2003;5(3):155-64.
27. Saeedi BJ, Kao DJ, Kitzenberg DA, Dobrinskikh E, Schwisow KD, Masterson JC, et al. HIF-dependent regulation of claudin-1 is central to intestinal epithelial tight junction integrity. *Mol Biol Cell*. 2015;26(12):2252-62.
28. Vouret-Craviari V, Boquet P, Pouysségur J, Van Obberghen-Schilling E. Regulation of the actin cytoskeleton by thrombin in human endothelial cells: role of Rho proteins in endothelial barrier function. *Mol Biol Cell*. 1998;9(9):2639-53.

29. Lennon PF, Taylor CT, Stahl GL, Colgan SP. Neutrophil-derived 5'-adenosine monophosphate promotes endothelial barrier function via CD73-mediated conversion to adenosine and endothelial A2B receptor activation. *J Exp Med*. 1998;188(8):1433-43.
30. van de Water FM, Boleij JM, Peters JGP, Russel FGM, Masereeuw R. Characterization of P-glycoprotein and multidrug resistance proteins in rat kidney and intestinal cell lines. *Eur J Pharm Sci*. 2007;30(1):36-44.
31. Jansen J, Schophuizen CM, Wilmer MJ, Lahham SH, Mutsaers HA, Wetzels JF, et al. A morphological and functional comparison of proximal tubule cell lines established from human urine and kidney tissue. *Exp Cell Res*. 2014;323(1):87-99.
32. Jouan E, Le Vee M, Denizot C, Da Violante G, Fardel O. The mitochondrial fluorescent dye rhodamine 123 is a high-affinity substrate for organic cation transporters (OCTs) 1 and 2. *Fundam Clin Pharmacol*. 2014;28(1):65-77.
33. Yumoto R, Murakami T, Nakamoto Y, Hasegawa R, Nagai J, Takano M. Transport of rhodamine 123, a P-glycoprotein substrate, across rat intestine and Caco-2 cell monolayers in the presence of cytochrome P-450 3A-related compounds. *J Pharmacol Exp Ther*. 1999;289(1):149-55.
34. Forster S, Thumser AE, Hood SR, Plant N. Characterization of rhodamine-123 as a tracer dye for use in in vitro drug transport assays. *PLoS One*. 2012;7(3):e33253-e.
35. Jouan E, Le Vée M, Mayati A, Denizot C, Parmentier Y, Fardel O. Evaluation of P-Glycoprotein Inhibitory Potential Using a Rhodamine 123 Accumulation Assay. *Pharmaceutics*. 2016;8(2):12.
36. Christensen EI, Birn H. Megalin and cubilin: multifunctional endocytic receptors. *Nat Rev Mol Cell Biol*. 2002;3(4):258-67.
37. Schuh CD, Polesel M, Platonova E, Haenni D, Gassama A, Tokonami N, et al. Combined Structural and Functional Imaging of the Kidney Reveals Major Axial Differences in Proximal Tubule Endocytosis. *J Am Soc Nephrol*. 2018;29(11):2696-712.
38. Schwegler JS, Heppelmann B, Mildenerger S, Silbernagl S. Receptor-mediated endocytosis of albumin in cultured opossum kidney cells: a model for proximal tubular protein reabsorption. *Pflugers Arch*. 1991;418(4):383-92.
39. Terryn S, Jouret F, Vandenabeele F, Smolders I, Moreels M, Devuyst O, et al. A primary culture of mouse proximal tubular cells, established on collagen-coated membranes. *Am J Physiol Renal Physiol*. 2007;293(2):476-85.
40. Raghavan V, Rbaibi Y, Pastor-Soler NM, Carattino MD, Weisz OA. Shear stress-dependent regulation of apical endocytosis in renal proximal tubule cells mediated by primary cilia. *Proc Natl Acad Sci U S A*. 2014;111(23):8506.
41. Shurety W, Stewart NL, Stow JL. Fluid-phase markers in the basolateral endocytic pathway accumulate in response to the actin assembly-promoting drug Jasplakinolide. *Mol Biol Cell*. 1998;9(4):957-75.

42. Dukes JD, Whitley P, Chalmers AD. The MDCK variety pack: choosing the right strain. *BMC Cell Biol.* 2011;12:43.
43. Hull RN, Cherry WR, Weaver GW. The origin and characteristics of a pig kidney cell strain, LLC-PK1. *In Vitro.* 1976;12(10):670-7.
44. Rabito CA. Occluding junctions in a renal cell line (LLC-PK1) with characteristics of proximal tubular cells. *Am J Physiol Renal Physiol.* 1986;250(4):734-43.
45. Leighton J, Estes LW, Mansukhani S, Brada Z. A cell line derived from normal dog kidney (MDCK) exhibiting qualities of papillary adenocarcinoma and of renal tubular epithelium. *Cancer.* 1970;26(5):1022-8.
46. Cereijido M, Robbins ES, Dolan WJ, Rotunno CA, Sabatini DD. Polarized monolayers formed by epithelial cells on a permeable and translucent support. *J Cell Biol.* 1978;77(3):853-80.
47. Hidalgo IJ, Raub TJ, Borchardt RT. Characterization of the human colon carcinoma cell line (Caco-2) as a model system for intestinal epithelial permeability. *Gastroenterology.* 1989;96(3):736-49.
48. Drummond CG, Nickerson CA, Coyne CB. A Three-Dimensional Cell Culture Model To Study Enterovirus Infection of Polarized Intestinal Epithelial Cells. *mSphere.* 2016;1(1):e00030-15.
49. Zhao L, Imperiale MJ. Establishing Renal Proximal Tubule Epithelial-Derived Cell Lines Expressing Human Telomerase Reverse Transcriptase for Studying BK Polyomavirus. *Microbiol Resour Announc.* 2019;8(42).
50. Secker PF, Luks L, Schlichenmaier N, Dietrich DR. RPTEC/TERT1 cells form highly differentiated tubules when cultured in a 3D matrix. *Altex.* 2018;35(2):223-34.
51. Wilmer MJ, Saleem MA, Masereeuw R, Ni L, van der Velden TJ, Russel FG, et al. Novel conditionally immortalized human proximal tubule cell line expressing functional influx and efflux transporters. *Cell Tissue Res.* 2010;339(2):449-57.
52. Di Mise A, Tamma G, Ranieri M, Svelto M, Heuvel Bvd, Levchenko EN, et al. Conditionally immortalized human proximal tubular epithelial cells isolated from the urine of a healthy subject express functional calcium-sensing receptor. *Am J Physiol Renal Physiol.* 2015;308(11):1200-06.
53. Lonza. Clonetics renal epithelial cell systems [Web page]. [Available from: [https://bioscience.lonza.com/lonza\\_bs/CH/en/download/product/asset/28070](https://bioscience.lonza.com/lonza_bs/CH/en/download/product/asset/28070)].
54. ScienCell Research Laboratories. Human Renal Proximal Tubular Epithelial Cell [Web page]. [Available from: <https://www.sciencellonline.com/PS/4100.pdf>].
55. Oosterwijk E, Muijen GNP, Oosterwijk-Wakka J, Warnaar S. Expression of intermediate filaments in developing and adult human kidney and in renal cell carcinoma. *The journal of histochemistry and cytochemistry : official journal of the Histochemistry Society.* 1990;38:385-92.

56. Nanus DM, Ebrahim SA, Bander NH, Real FX, Pfeffer LM, Shapiro JR, et al. Transformation of human kidney proximal tubule cells by ras-containing retroviruses. Implications for tumor progression. *The Journal of experimental medicine*. 1989;169(3):953-72.
57. Qi W, Johnson DW, Vesey DA, Pollock CA, Chen X. Isolation, propagation and characterization of primary tubule cell culture from human kidney (*Methods in Renal Research*). *Nephrology*. 2007;12(2):155-9.
58. Trifillis AL, Regec AL, Trump BF. Isolation, culture and characterization of human renal tubular cells. *The Journal of urology*. 1985;133(2):324-9.
59. Humes HD, Fissell WH, Weitzel WF, Buffington DA, Westover AJ, MacKay SM, et al. Metabolic replacement of kidney function in uremic animals with a bioartificial kidney containing human cells. *Am J Kidney Dis*. 2002;39(5):1078-87.
60. Johnson DW, Brew BK, Poronnik P, Cook DI, GyÖRy AZ, Field MJ, et al. Transport characteristics of human proximal tubule cells in primary culture. *Nephrology*. 1997;3(2):183-94.
61. Detrisac CJ, Sens MA, Garvin AJ, Spicer SS, Sens DA. Tissue culture of human kidney epithelial cells of proximal tubule origin. *Kidney Int*. 1984;25(2):383-90.
62. Rahmoune H, Thompson PW, Ward JM, Smith CD, Hong G, Brown J. Glucose Transporters in Human Renal Proximal Tubular Cells Isolated From the Urine of Patients With Non-Insulin-Dependent Diabetes. *Diabetes*. 2005;54(12):3427-34.
63. Zhou T, Benda C, Dunzinger S, Huang Y, Ho JC, Yang J, et al. Generation of human induced pluripotent stem cells from urine samples. *Nat Protoc*. 2012;7:2080-9.
64. Dorrenhaus A, Muller JI, Golka K, Jedrusik P, Schulze H, Follmann W. Cultures of exfoliated epithelial cells from different locations of the human urinary tract and the renal tubular system. *Arch Toxicol*. 2000;74(10):618-26.
65. Hasan S, Sebo P, Osicka R. A guide to polarized airway epithelial models for studies of host-pathogen interactions. *FEBS J*. 2018;285(23):4343-58.
66. Bryant DM, Mostov KE. From cells to organs: building polarized tissue. *Nat Rev Mol Cell Biol*. 2008;9:887.
67. Huh D, Hamilton GA, Ingber DE. From 3D cell culture to organs-on-chips. *Trends Cell Biol*. 2011;21(12):745-54.
68. Kauffman A, Gyurdieva A, Mabus J, Ferguson C, Yan Z, Hornby P. Alternative functional in vitro models of human intestinal epithelia. *Front Pharmacol*. 2013;4(79).
69. Nishinakamura R. Human kidney organoids: progress and remaining challenges. *Nat Rev Nephrol*. 2019;15(10):613-24.
70. Gozalpour E, Fenner KS. Current State of In vitro Cell-Based Renal Models. *Curr Drug Metab*. 2018;19(4):310-26.

71. Rindler MJ, Chuman LM, Shaffer L, Saier MH. Retention of differentiated properties in an established dog kidney epithelial cell line (MDCK). *J Cell Biol.* 1979;81(3):635-48.
72. Ryan MJ, Johnson G, Kirk J, Fuerstenberg SM, Zager RA, Torok-Storb B. HK-2: An immortalized proximal tubule epithelial cell line from normal adult human kidney. *Kidney Int.* 1994;45(1):48-57.
73. Taub M, Sato G. Growth of functional primary cultures of kidney epithelial cells in defined medium. *J Cell Physiol.* 1980;105(2):369-78.
74. Justice BA, Badr NA, Felder RA. 3D cell culture opens new dimensions in cell-based assays. *Drug Discov Today.* 2009;14(1-2):102-7.
75. Fulcher ML, Gabriel S, Burns KA, Yankaskas JR, Randell SH. Well-Differentiated Human Airway Epithelial Cell Cultures. In: Picot J, editor. *Human Cell Culture Protocols.* Totowa, NJ: Humana Press; 2005. p. 183-206.
76. Sonoda S, Spee C, Barron E, Ryan SJ, Kannan R, Hinton DR. A protocol for the culture and differentiation of highly polarized human retinal pigment epithelial cells. *Nat Protoc.* 2009;4:662-73.
77. Balcarova-Ständer J, Pfeiffer SE, Fuller SD, Simons K. Development of cell surface polarity in the epithelial Madin-Darby canine kidney (MDCK) cell line. *EMBO J.* 1984;3(11):2687-94.
78. Courjault-Gautier F, Chevalier J, Abbou CC, Chopin DK, Toutain HJ. Consecutive use of hormonally defined serum-free media to establish highly differentiated human renal proximal tubule cells in primary culture. *J Am Soc Nephrol.* 1995;5(11):1949-63.
79. Hoppensack A, Kazanecki CC, Colter D, Gosiewska A, Schanz J, Walles H, et al. A human in vitro model that mimics the renal proximal tubule. *Tissue engineering Part C, Methods.* 2014;20(7):599-609.
80. Van der Hauwaert C, Savary G, Gnemmi V, Glowacki F, Pottier N, Bouillez A, et al. Isolation and characterization of a primary proximal tubular epithelial cell model from human kidney by CD10/CD13 double labeling. *PLoS One.* 2013;8(6):e66750-e.
81. Ferrell N, Cheng J, Miao S, Roy S, Fissell WH. Orbital Shear Stress Regulates Differentiation and Barrier Function of Primary Renal Tubular Epithelial Cells. *ASAIO J.* 2018;64(6):766-72.
82. Jalal F, Dehbi M, Berteloot A, Crine P. Biosynthesis and polarized distribution of neutral endopeptidase in primary cultures of kidney proximal tubule cells. *Biochem J.* 1994;302 ( Pt 3)(Pt 3):669-74.
83. Blais A, Jalal F, Crine P, Paiement J, Berteloot A. Increased functional differentiation of rabbit proximal tubule cells cultured in glucose-free media. *Am J Physiol.* 1992;263(1):152-62.
84. Blackburn JG, Hazen-Martin DJ, Detrisac CJ, Sens DA. Electrophysiology and ultrastructure of cultured human proximal tubule cells. *Kidney Int.* 1988;33(2):508-16.

85. Tavelin S, Gråsjö J, Taipalensuu J, Ocklind G, Artursson P. Applications of Epithelial Cell Culture in Studies of Drug Transport. In: Wise C, editor. *Epithelial Cell Culture Protocols*. Totowa, NJ: Humana Press; 2002. p. 233-72.
86. Clayson ET, Compans RW. Entry of simian virus 40 is restricted to apical surfaces of polarized epithelial cells. *Mol Cell Biol*. 1988;8(8):3391-6.
87. Finlay BB, Falkow S. Salmonella interactions with polarized human intestinal Caco-2 epithelial cells. *J Infect Dis*. 1990;162(5):1096-106.
88. Bhatia SN, Ingber DE. Microfluidic organs-on-chips. *Nat Biotechnol*. 2014;32(8):760-72.
89. Clevers H. Modeling Development and Disease with Organoids. *Cell*. 2016;165(7):1586-97.
90. Clayson ET, Brando LV, Compans RW. Release of simian virus 40 virions from epithelial cells is polarized and occurs without cell lysis. *J Virol*. 1989;63(5):2278-88.
91. Rinaldo CH, Tylden GD, Sharma BN. The human polyomavirus BK (BKPyV): virological background and clinical implications. *APMIS*. 2013;121(8):728-45.
92. Belouzard S, Danneels A, Fénéant L, Séron K, Rouillé Y, Dubuisson J. Entry and Release of Hepatitis C Virus in Polarized Human Hepatocytes. *J Virol*. 2017;91(18).
93. Capelli N, Marion O, Dubois M, Allart S, Bertrand-Michel J, Lhomme S, et al. Vectorial Release of Hepatitis E Virus in Polarized Human Hepatocytes. *J Virol*. 2019;93(4).
94. Tamhankar M, Patterson JL. Directional entry and release of Zika virus from polarized epithelial cells. *Virol J*. 2019;16(1):99.
95. Hierholzer JC, Castells E, Banks GG, Bryan JA, McEwen CT. Sensitivity of NCI-H292 human lung mucoepidermoid cells for respiratory and other human viruses. *J Clin Microbiol*. 1993;31(6):1504-10.
96. Katoh H, Nakatsu Y, Kubota T, Sakata M, Takeda M, Kidokoro M. Mumps Virus Is Released from the Apical Surface of Polarized Epithelial Cells, and the Release Is Facilitated by a Rab11-Mediated Transport System. *J Virol*. 2015;89(23):12026-34.
97. Schlie K, Maisa A, Freiberg F, Groseth A, Strecker T, Garten W. Viral protein determinants of Lassa virus entry and release from polarized epithelial cells. *J Virol*. 2010;84(7):3178-88.
98. Cordo SM, Acuña MCY, Candurra NA. Polarized entry and release of Junin virus, a New World arenavirus. *J Gen Virol*. 2005;86(5):1475-9.
99. Connolly-Andersen AM, Magnusson KE, Mirazimi A. Basolateral entry and release of Crimean-Congo hemorrhagic fever virus in polarized MDCK-1 cells. *J Virol*. 2007;81(5):2158-64.
100. Lamp B, Dietzel E, Kolesnikova L, Sauerhering L, Erbar S, Weingartl H, et al. Nipah virus entry and egress from polarized epithelial cells. *J Virol*. 2013;87(6):3143-54.

101. Krautkrämer E, Lehmann MJ, Bollinger V, Zeier M. Polar release of pathogenic Old World hantaviruses from renal tubular epithelial cells. *Virology*. 2012;9(1):299.
102. Low J, Humes HD, Szczypka M, Imperiale M. BKV and SV40 infection of human kidney tubular epithelial cells in vitro. *Virology*. 2004;323(2):182-8.
103. Morris-Love J, Gee GV, O'Hara BA, Assetta B, Atkinson AL, Dugan AS, et al. JC Polyomavirus Uses Extracellular Vesicles To Infect Target Cells. *mBio*. 2019;10(2):e00379-19.
104. Handala L, Blanchard E, Raynal P-I, Roingeard P, Morel V, Descamps V, et al. BK Polyomavirus Hijacks Extracellular Vesicles for En Bloc Transmission. *J Virol*. 2020;94(6):e01834-19.
105. Evans GL, Caller LG, Foster V, Crump CM. Anion homeostasis is important for non-lytic release of BK polyomavirus from infected cells. *Open Biol*. 2015;5(8).
106. Dumoulin A, Hirsch HH. Reevaluating and optimizing polyomavirus BK and JC real-time PCR assays to detect rare sequence polymorphisms. *J Clin Microbiol*. 2011;49(4):1382-8.
107. Cocchiario JL, Kumar Y, Fischer ER, Hackstadt T, Valdivia RH. Cytoplasmic lipid droplets are translocated into the lumen of the Chlamydia trachomatis parasitophorous vacuole. *Proc Natl Acad Sci U S A*. 2008;105(27):9379-84.
108. Pokrovskaya ID, Szwedlo JW, Goodwin A, Lupashina TV, Nagarajan UM, Lupashin VV. Chlamydia trachomatis hijacks intra-Golgi COG complex-dependent vesicle trafficking pathway. *Cell Microbiol*. 2012;14(5):656-68.
109. Rinaldo CH, Traavik T, Hey A. The agnogene of the human polyomavirus BK is expressed. *J Virol*. 1998;72(7):6233-6.
110. Hey AW, Johnsen JI, Johansen B, Traavik T. A two fusion partner system for raising antibodies against small immunogens expressed in bacteria. *J Immunol Methods*. 1994;173(2):149-56.
111. Desai RA, Gao L, Raghavan S, Liu WF, Chen CS. Cell polarity triggered by cell-cell adhesion via E-cadherin. *J Cell Sci*. 2009;122(7):905-11.
112. Tucker SP, Thornton CL, Wimmer E, Compans RW. Vectorial release of poliovirus from polarized human intestinal epithelial cells. *J Virol*. 1993;67(7):4274-82.
113. Inoue CN, Sunagawa N, Morimoto T, Ohnuma S, Katsushima F, Nishio T, et al. Reconstruction of tubular structures in three-dimensional collagen gel culture using proximal tubular epithelial cells voided in human urine. *In Vitro Cell Dev Biol Anim*. 2003;39:364-7.
114. Felix JS, Sun TT, Littlefield JW. Human epithelial cells cultured from urine: growth properties and keratin staining. *In Vitro*. 1980;16(10):866-74.
115. Helle F, Brochot E, Handala L, Martin E, Castelain S, Francois C, et al. Biology of the BKPyV: An Update. *Viruses*. 2017;9(11):327.



116. Mee CJ, Grove J, Harris HJ, Hu K, Balfe P, McKeating JA. Effect of cell polarization on hepatitis C virus entry. *J Virol*. 2008;82(1):461-70.
117. Lim PJ, Chu JJH. A Polarized Cell Model for Chikungunya Virus Infection: Entry and Egress of Virus Occurs at the Apical Domain of Polarized Cells. *PLoS Negl Trop Dis*. 2014;8(2):e2661.
118. Morshed KM, McMartin KE. Transient alterations in cellular permeability in cultured human proximal tubule cells: implications for transport studies. *In Vitro Cell Dev Biol Anim*. 1995;31(2):107-14.
119. Elwi AN, Damaraju VL, Kuzma ML, Mowles DA, Baldwin SA, Young JD, et al. Transepithelial fluxes of adenosine and 2'-deoxyadenosine across human renal proximal tubule cells: roles of nucleoside transporters hENT1, hENT2, and hCNT3. *Am J Physiol Renal Physiol*. 2009;296(6):1439-51.
120. Ronco P, Antoine M, Baudouin B, Geniteau-legendre M, Lelongt B, Chatelet F, et al. Polarized membrane expression of brush-border hydrolases in primary cultures of kidney proximal tubular cells depends on cell differentiation and is induced by dexamethasone. *J Cell Physiol*. 1990;145(2):222-37.

# Illustrations and figures

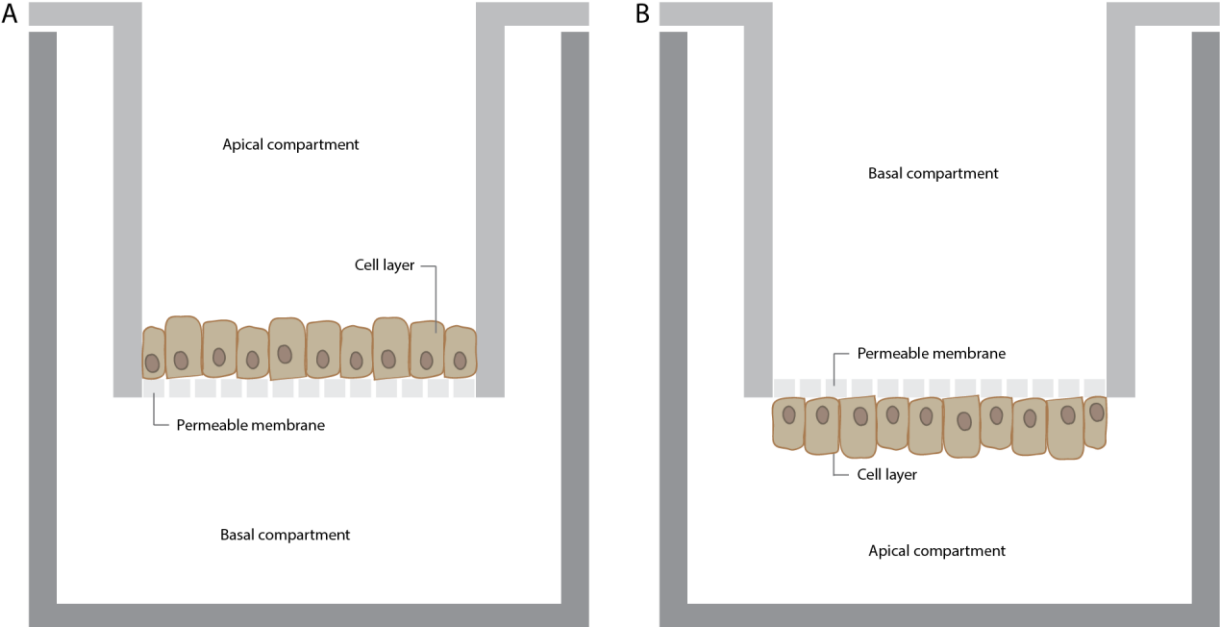
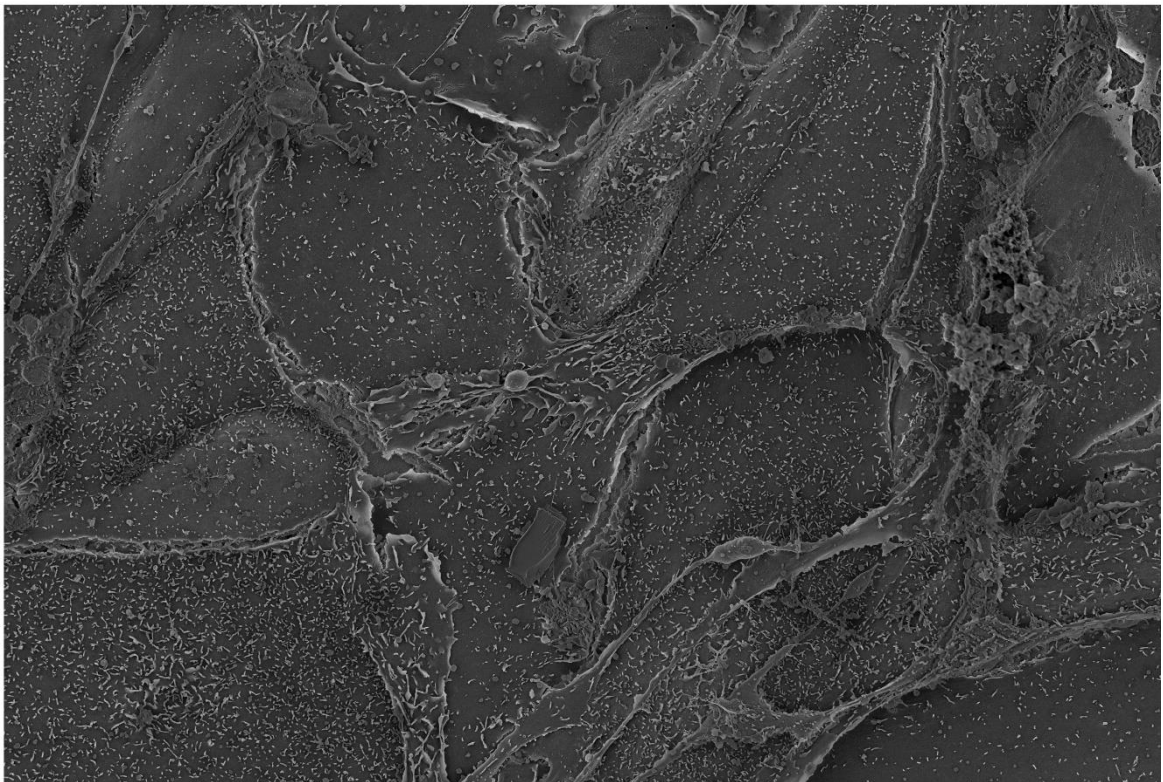
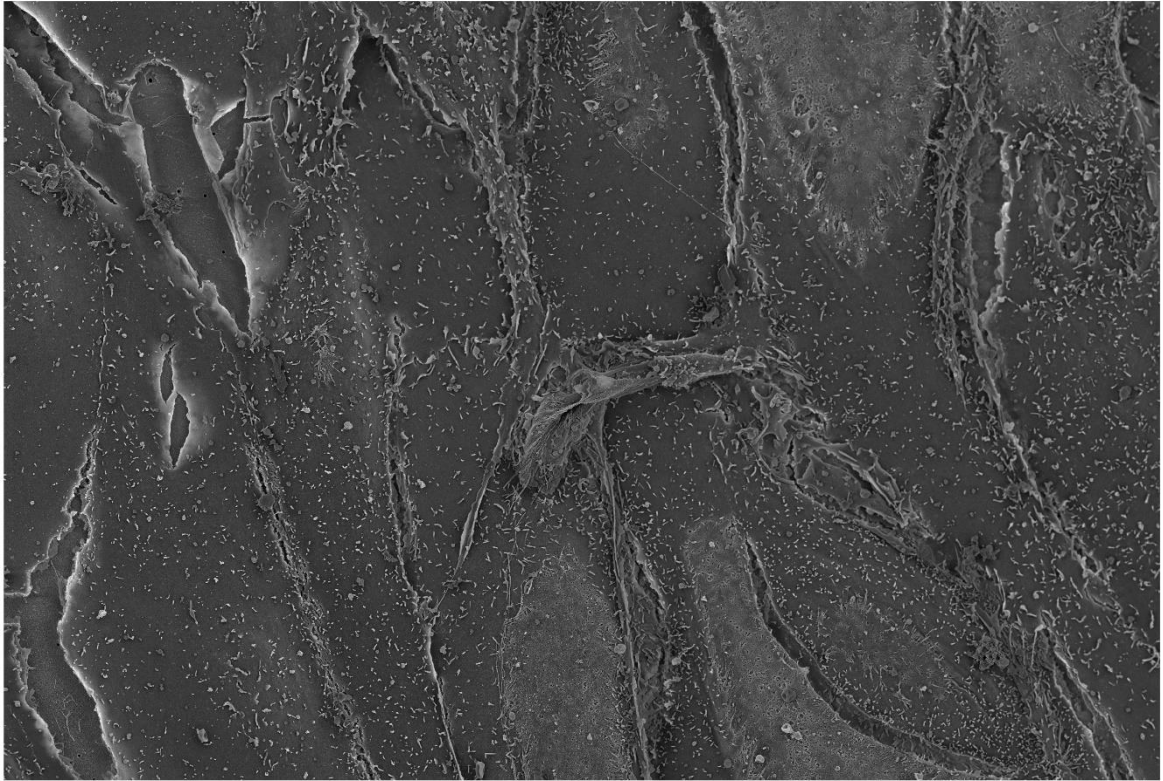
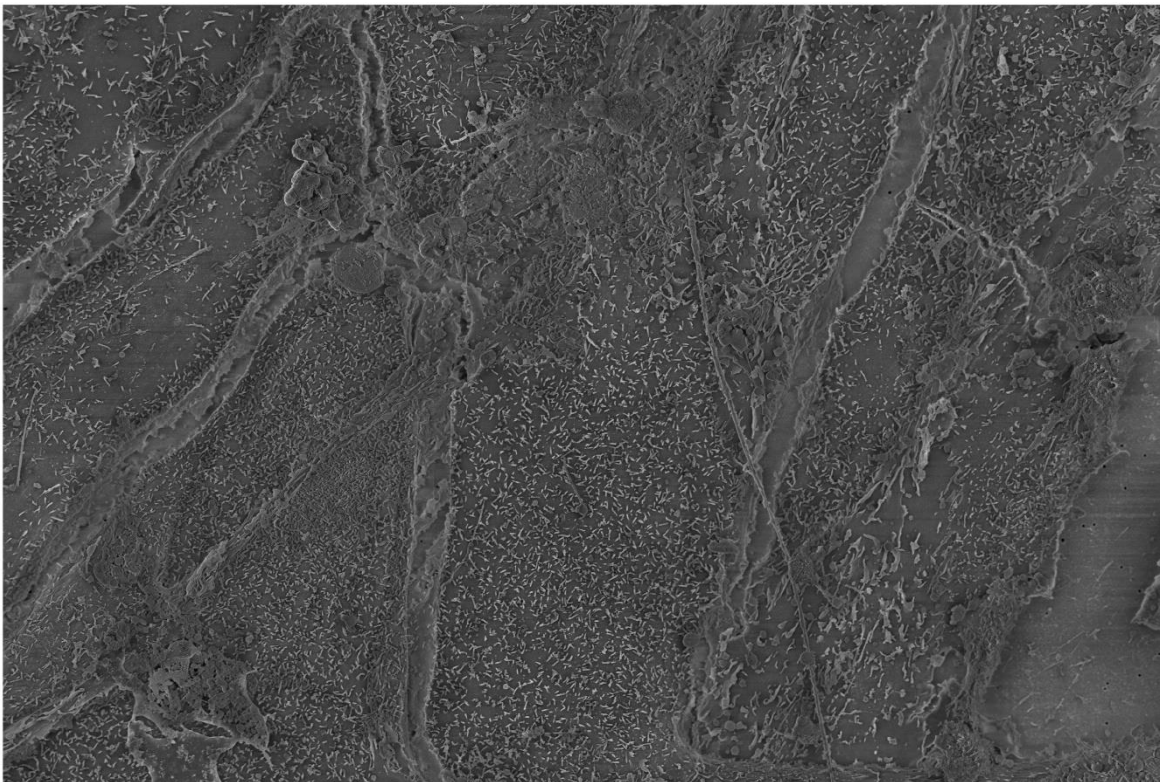
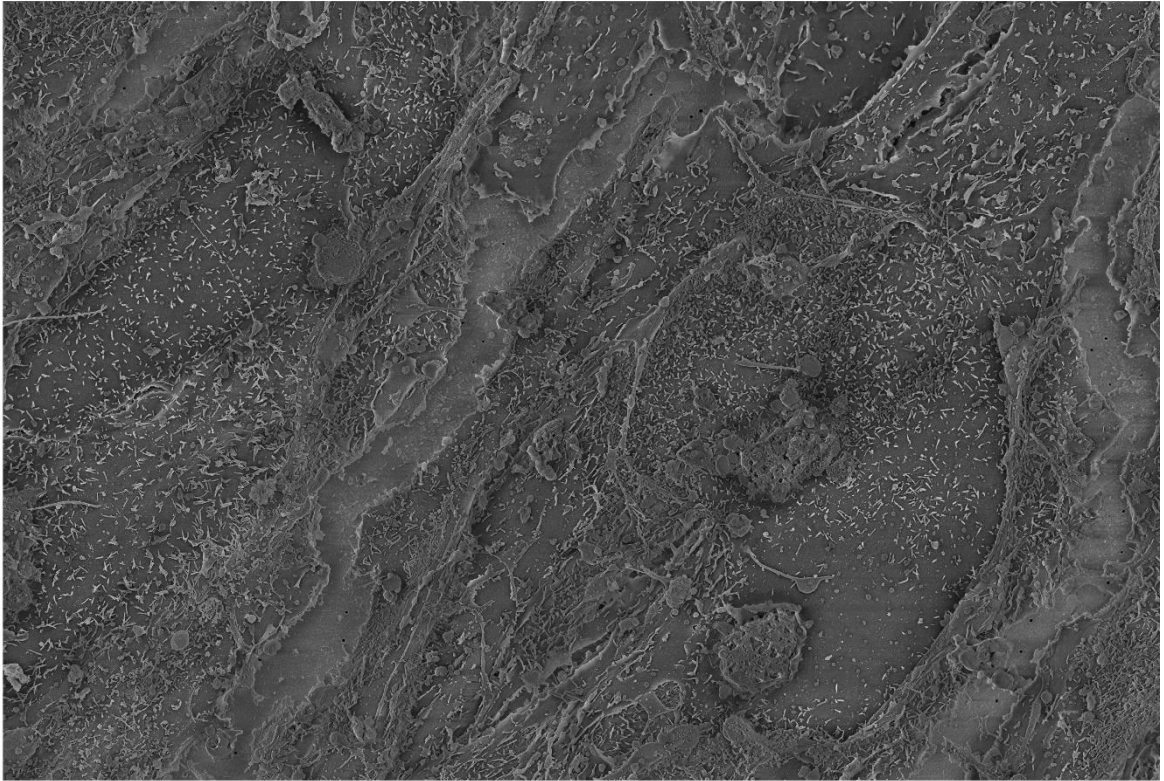


**Illustration 1.** Illustration of cells seeded on a permeable support. Cells can be seeded inside the support (A) or on the underside of the support (B).

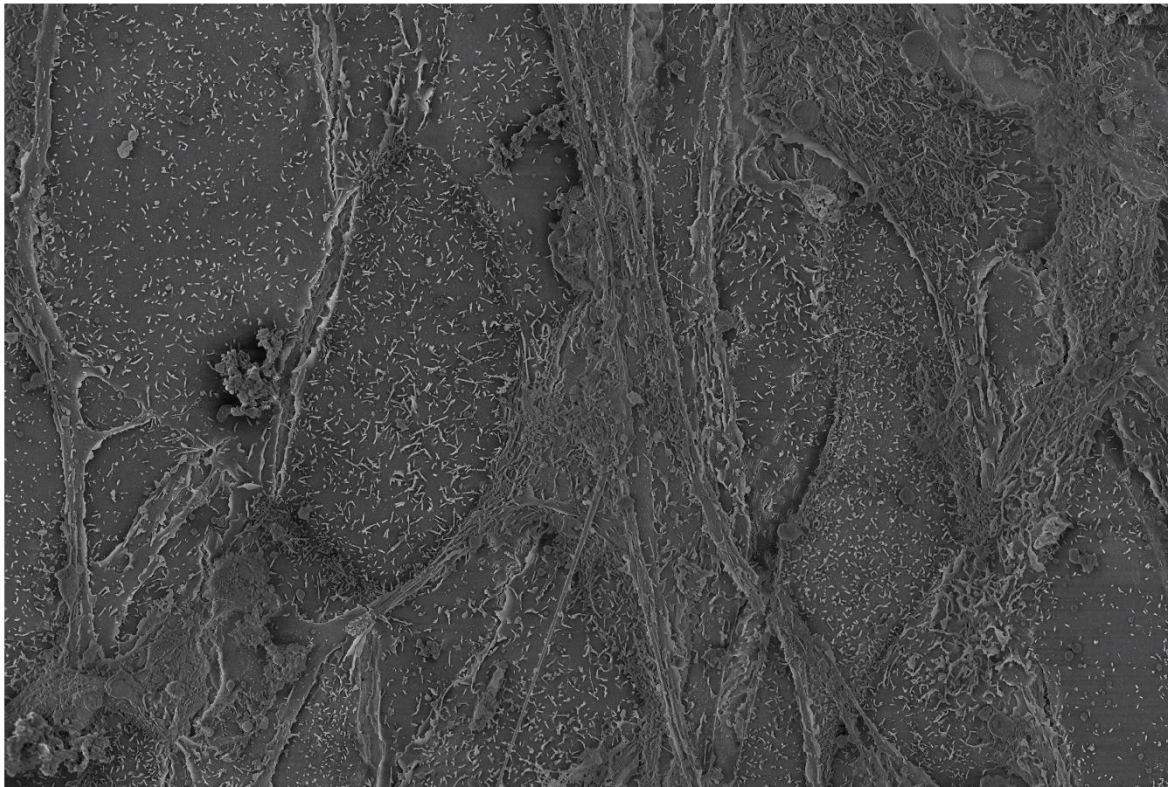
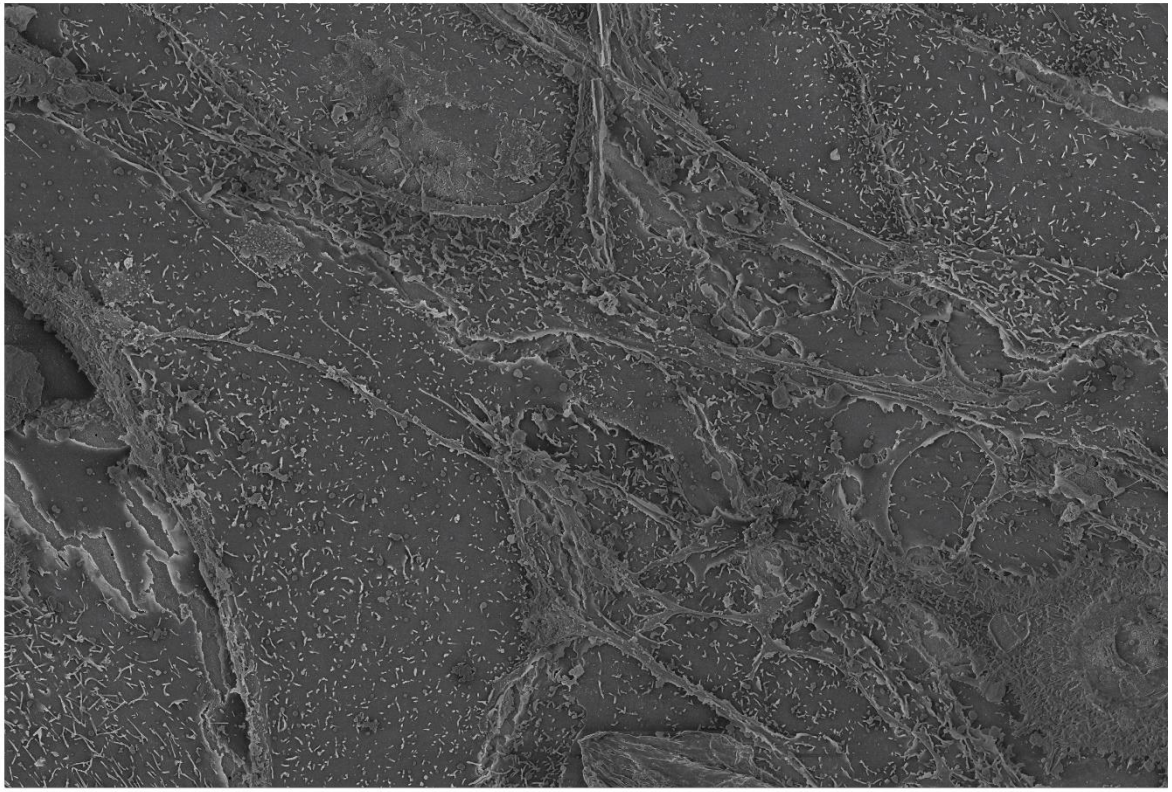
A



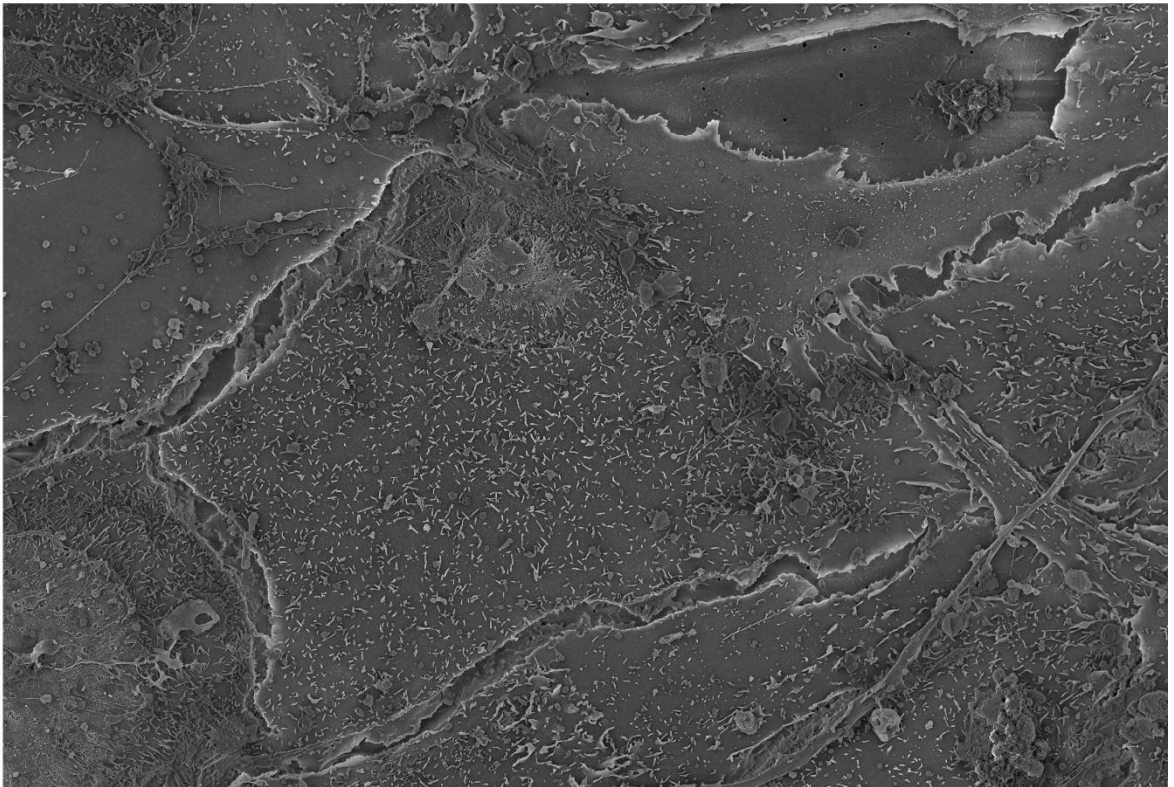
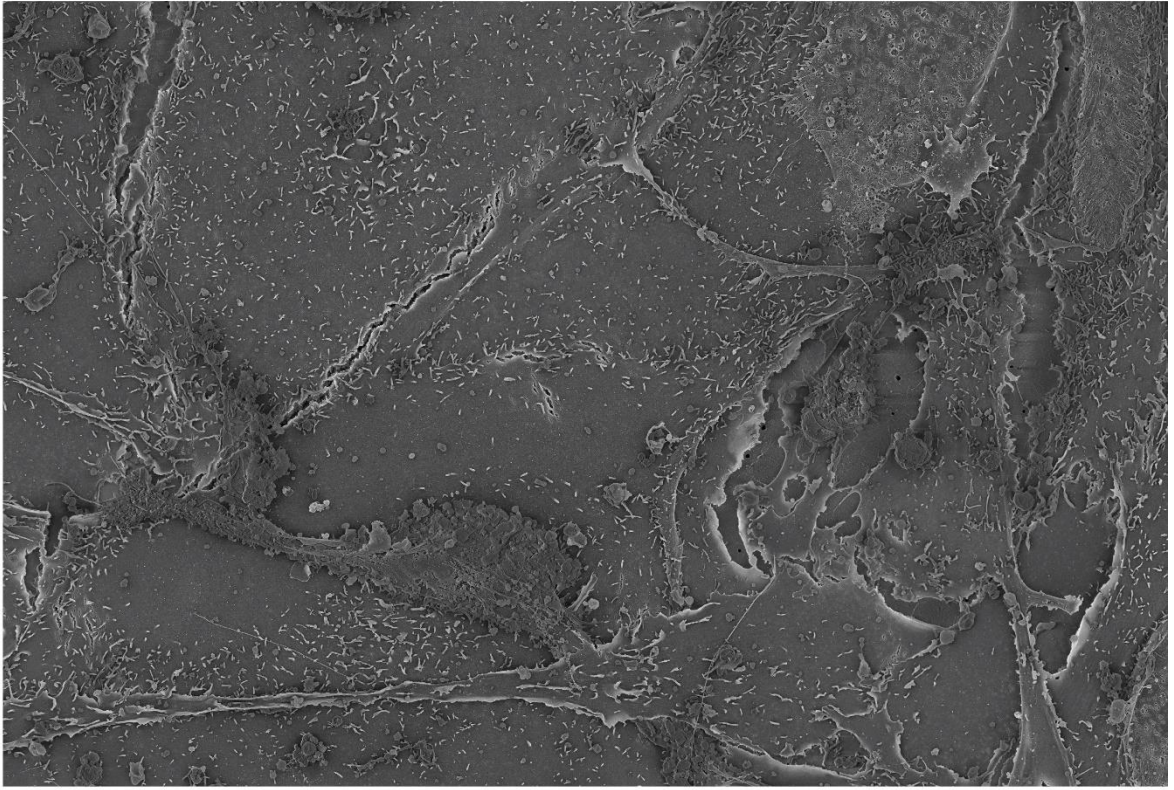
B



C



D



E

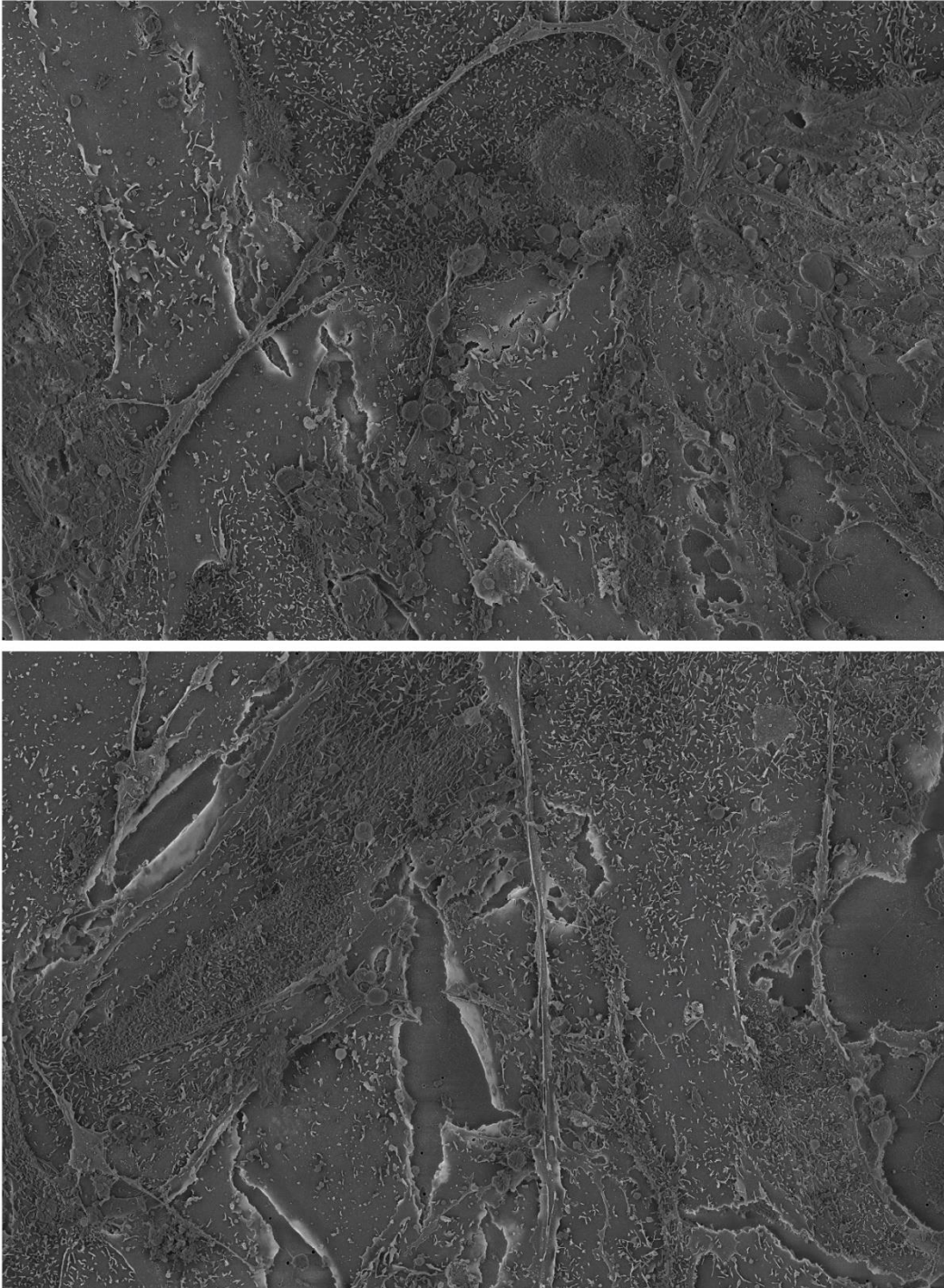


**Figure 1: Adult RPTeCs have microvilli**

SEM of adult RPTeCs. **A:** RPTeCs cultured for three days exhibited microvilli prior to differentiation. **B:** Adult RPTeCs differentiated for seven days confirms that differentiation leads to an increased number of microvilli. **C-E:** Adult RPTeCs cultured for ten, 14 and 17 days, respectively, retain microvilli as shown by SEM. All images are representative images of two experiments.

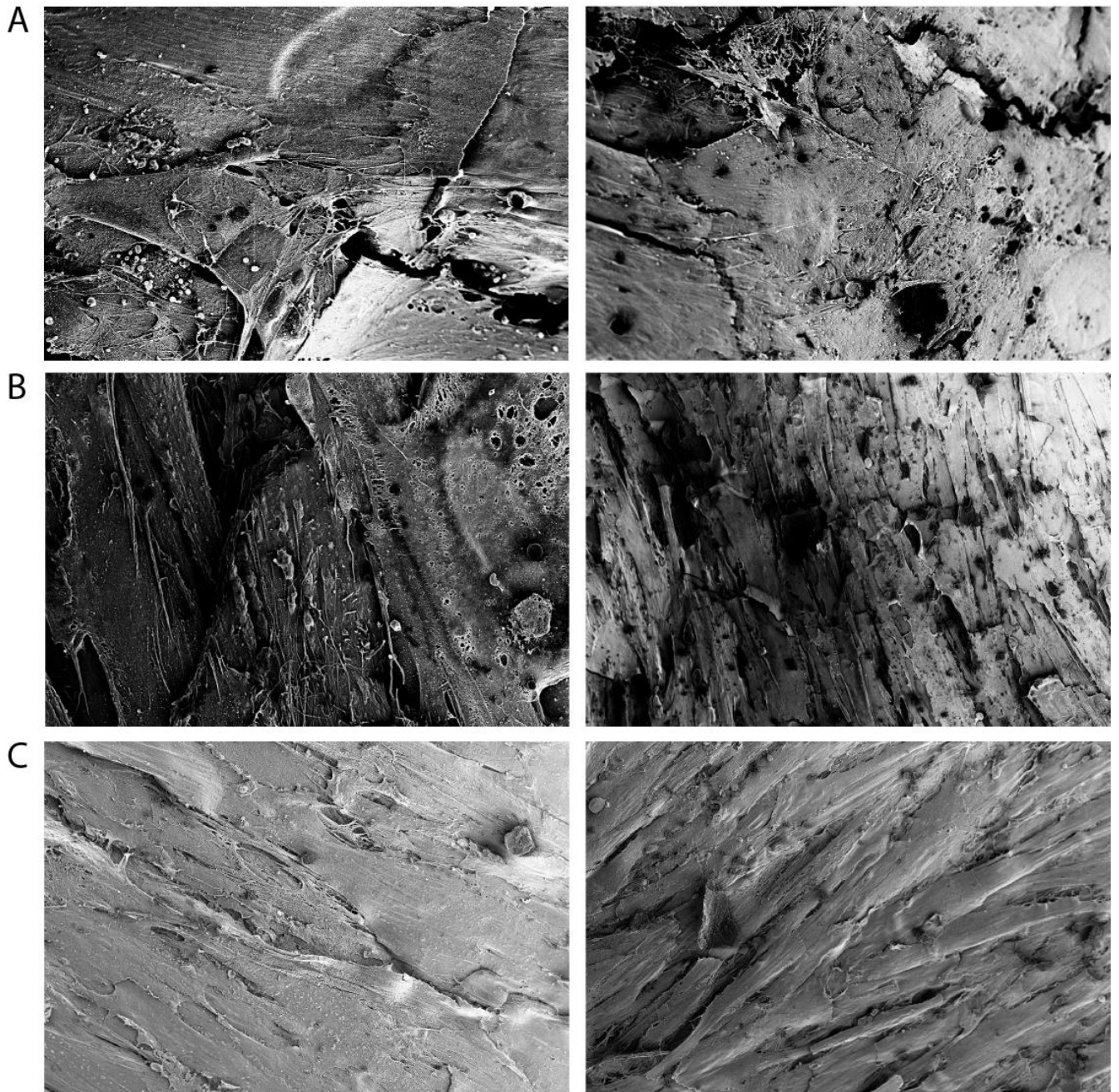


**Figure 2: Fetal RPTEC do not develop microvilli**

SEM of fetal and fetal RPTECs. **A:** Fetal RPTECs cultured for three days display no microvilli.

**B-C:** After 14 days and 20 days of culture, respectively, microvilli are still not present. All images are representative images of two experiments



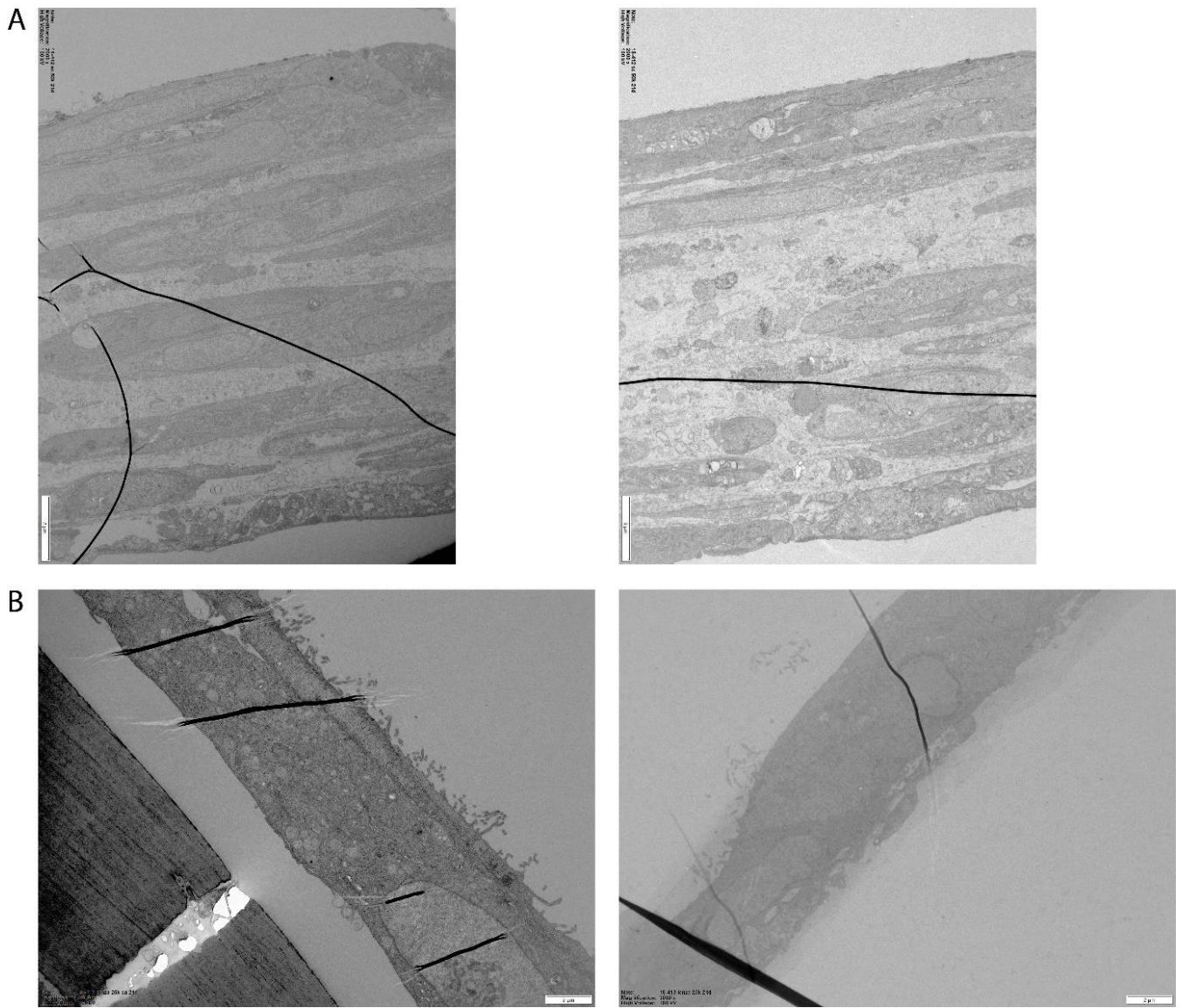


**Figure 3: Adult RPTECs develop a more polarized morphology compared to fetal RPTECs**

TEM of fetal and adult RPTECs after culture for 21 days. **A:** Fetal RPTECs demonstrates lack of microvilli and cells do not grow in a monolayer. **B:** Adult RPTECs developed microvilli and grow in a monolayer. Two representative images are of one experiment are shown.

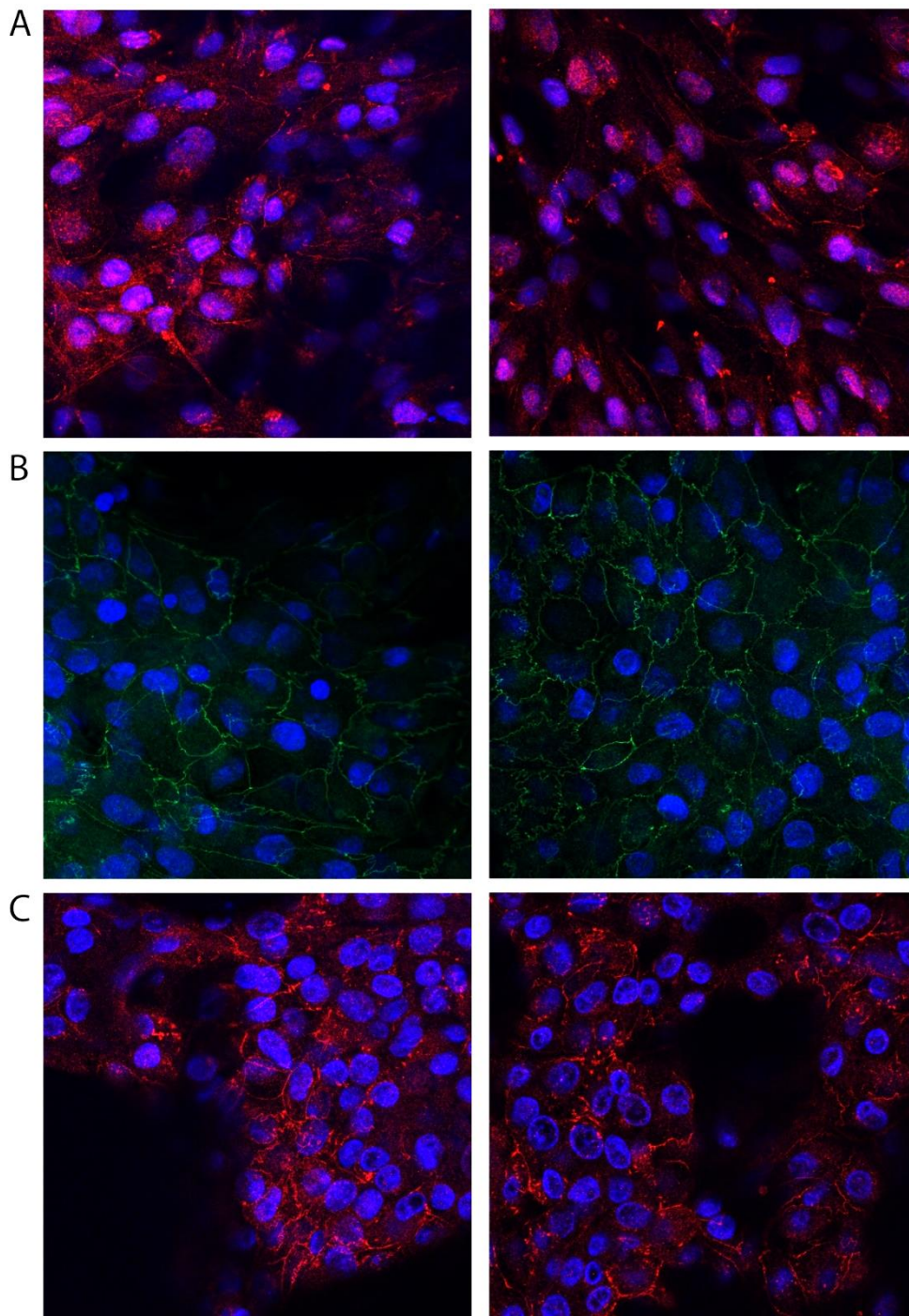


**Figure 4: Adult RPTECs develop tight junctions after differentiation**

IF microscopy of adult RPTECs stained for ZO-1 (red or green) in combination with the nuclei marker DRAQ5 (blue). **A:** After three days of culture, ZO-1 is diffusely distributed. **B:** At ten days of culture, an increased expression of ZO-1 along the lateral membranes was seen. **C:** After 14 days of culture, ZO-1 is strongly expressed at the lateral membranes. Two representative images of two experiments are shown.

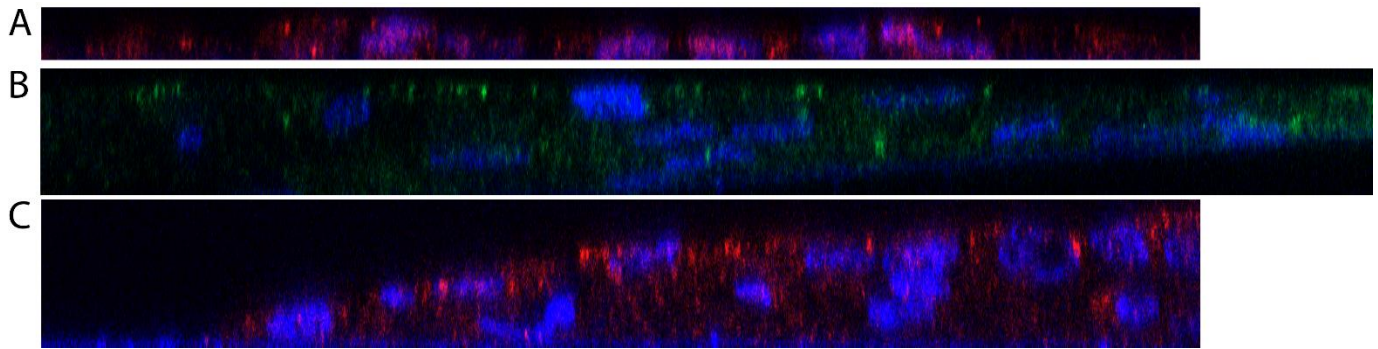


**Figure 5: Tight junctions are subapically located in adult RPTECs**

Lateral view of RPTECs stained for ZO-1 (red or green) and DRAQ5 (blue). **A:** Lateral view of ZO-1-stained adult RPTECs demonstrates subapical tight junctions before differentiation. **B:** After differentiation for ten days, subapical ZO-1 staining increases. **C:** 14 dps, RPTECs exhibit strong punctate staining of ZO-1. All images are representative images of two experiments.

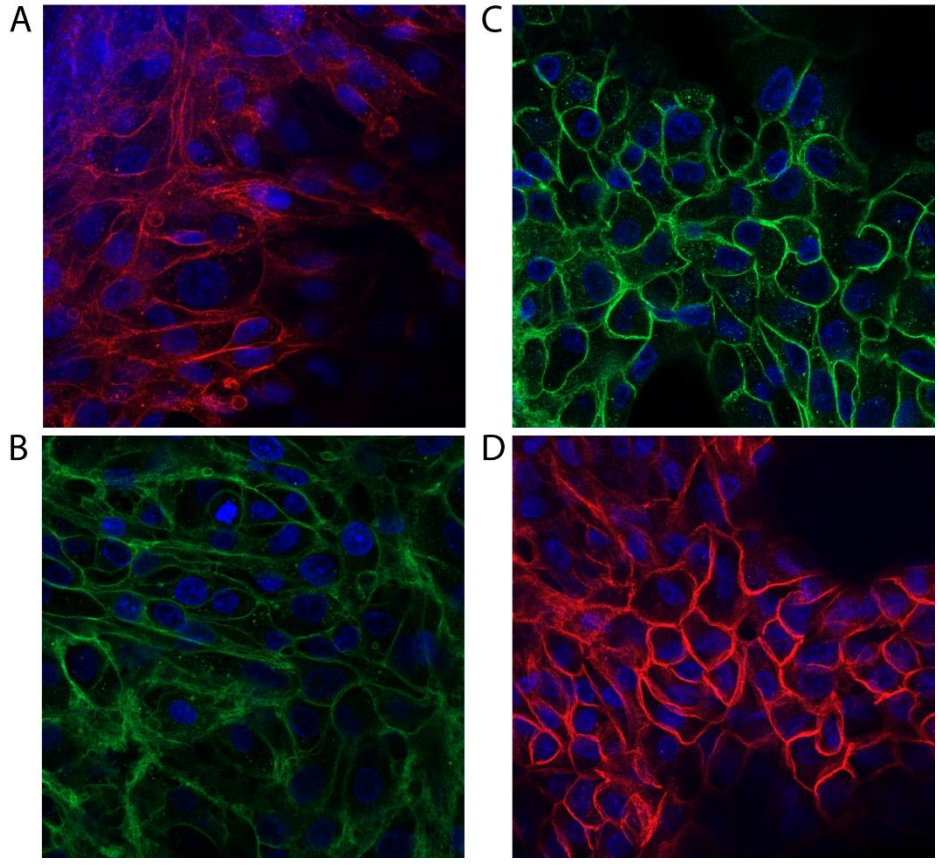


**Figure 6: Differentiation leads to lateral distribution of Na/K-ATPase in RPTECs**

IF microscopy of adult RPTECs stained for Na/K-ATPase (red or green) in combination with DRAQ5 (blue). **A:** IF staining of Na/K-ATPase and DRAQ5 demonstrates lateral and diffuse distribution of Na/K-ATPase three dps. **B, C and D:** After culture for eight, ten or 14 days, the Na/K-ATPase staining increased and was redistributed to the lateral membrane. All images are representative images of two experiments.

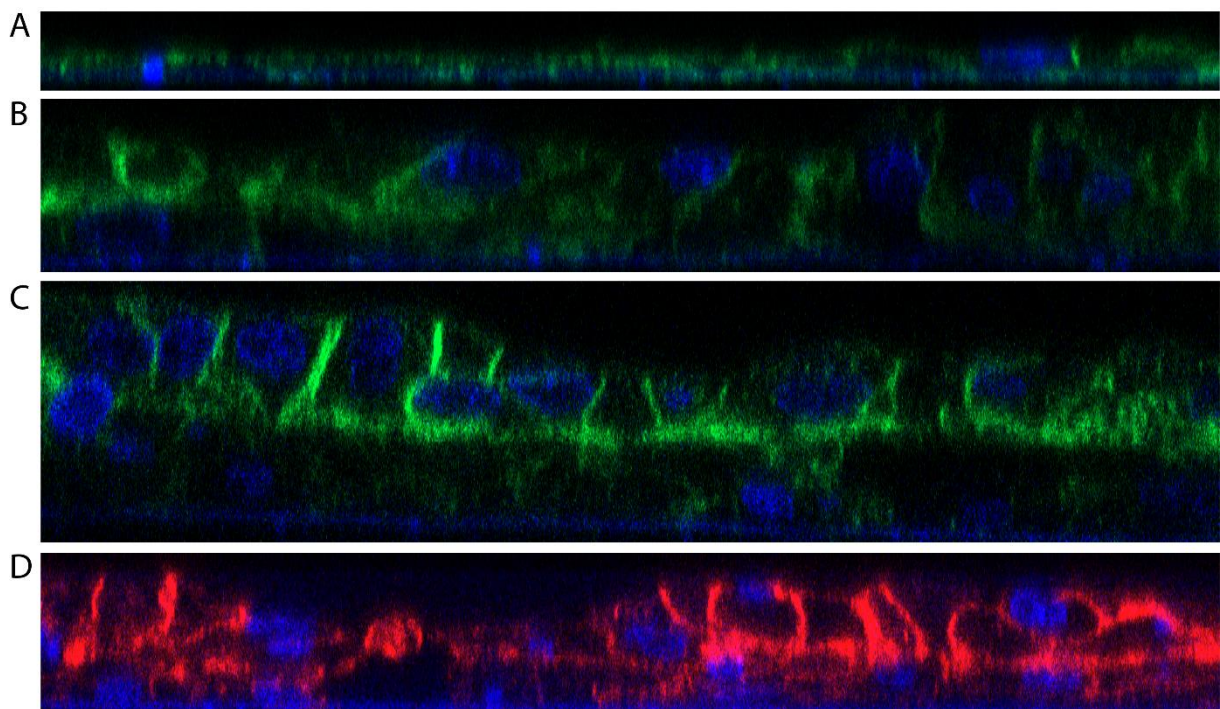


**Figure 7: Differentiation leads to basolateral distribution of Na/K-ATPase**

Lateral view of IF microscopy of adult RPTECs stained for Na/K-ATPase (red or green) in combination with DRAQ5 (blue). **A:** Three dps, Na/K-ATPase stained the whole plasma membrane of RPTECs. **B, C and D:** Eight, ten and 14 dps, Na/K-ATPase was restricted to the basolateral membrane of RPTECs. All images are representative images of two experiments.

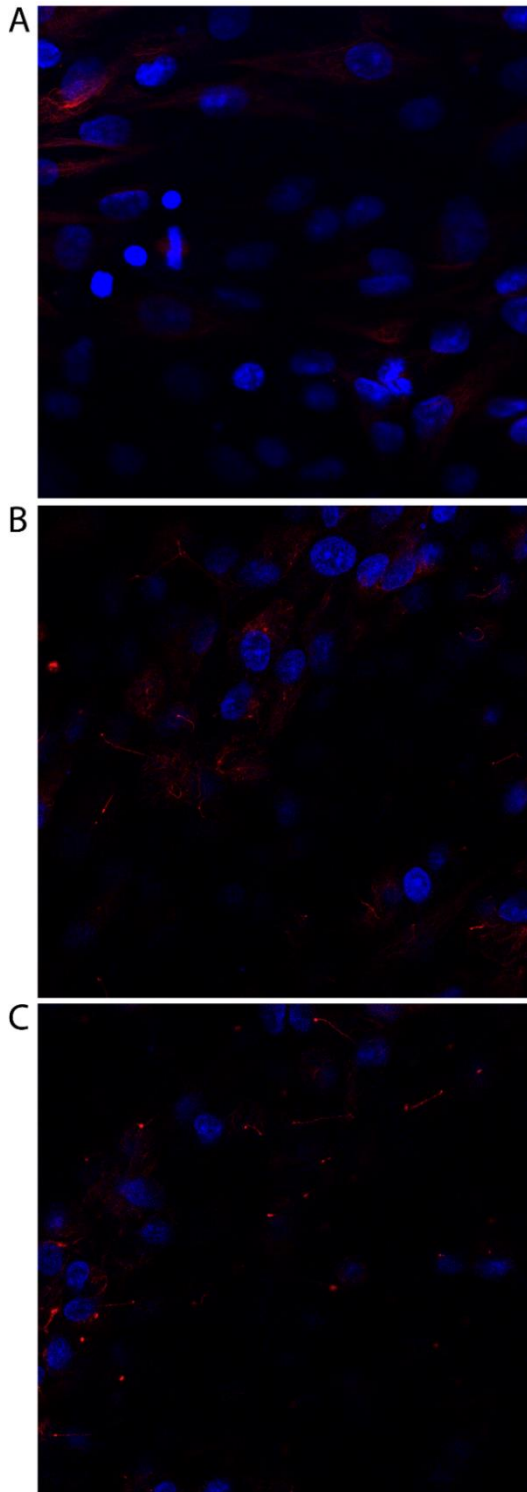


**Figure 8: RPTECs develop primary cilia during differentiation**

IF microscopy of adult RPTECs stained for acetylated tubulin (red) in combination with DRAQ5 (blue) **A:** Three dps, IF of acetylated tubulin demonstrate lack of primary cilia in RPTECs before differentiation. **B and C:** Eight and ten dps, primary cilia are present. All images are representative images of two experiments.

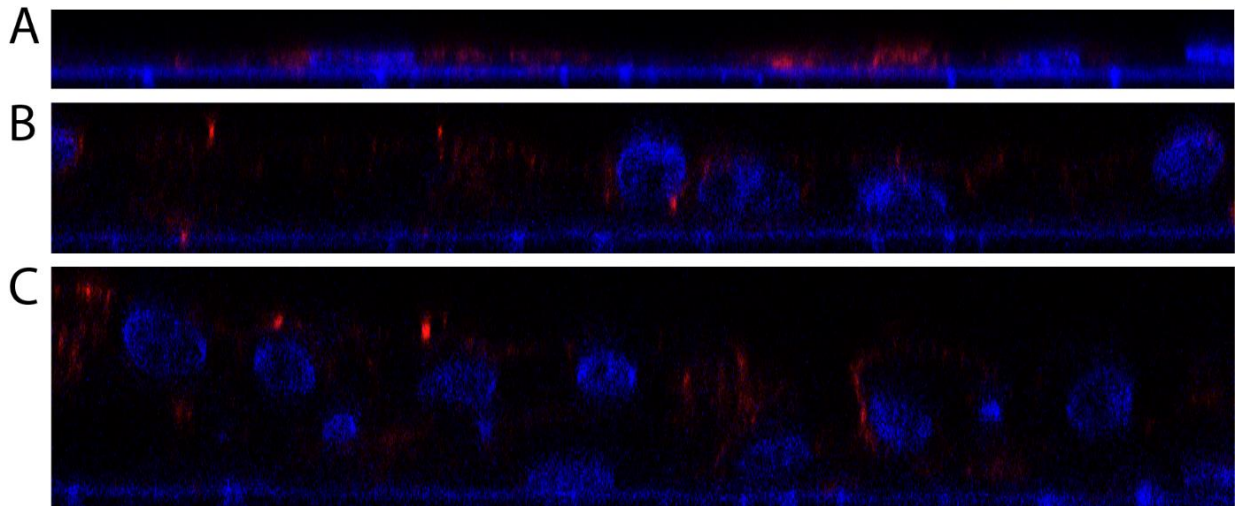


**Figure 9: Primary cilia extend from the apical membrane**

Lateral view of IF microscopy of adult RPTECs stained for acetylated tubulin (red) in combination with DRAQ5 (blue). **A:** Three dps, no RPTECs exhibited clear punctate staining of acetylated tubulin. **B and C:** Eight and ten dps, punctate staining of acetylated tubulin at the apical membrane was evident. All images are representative images of two experiments.

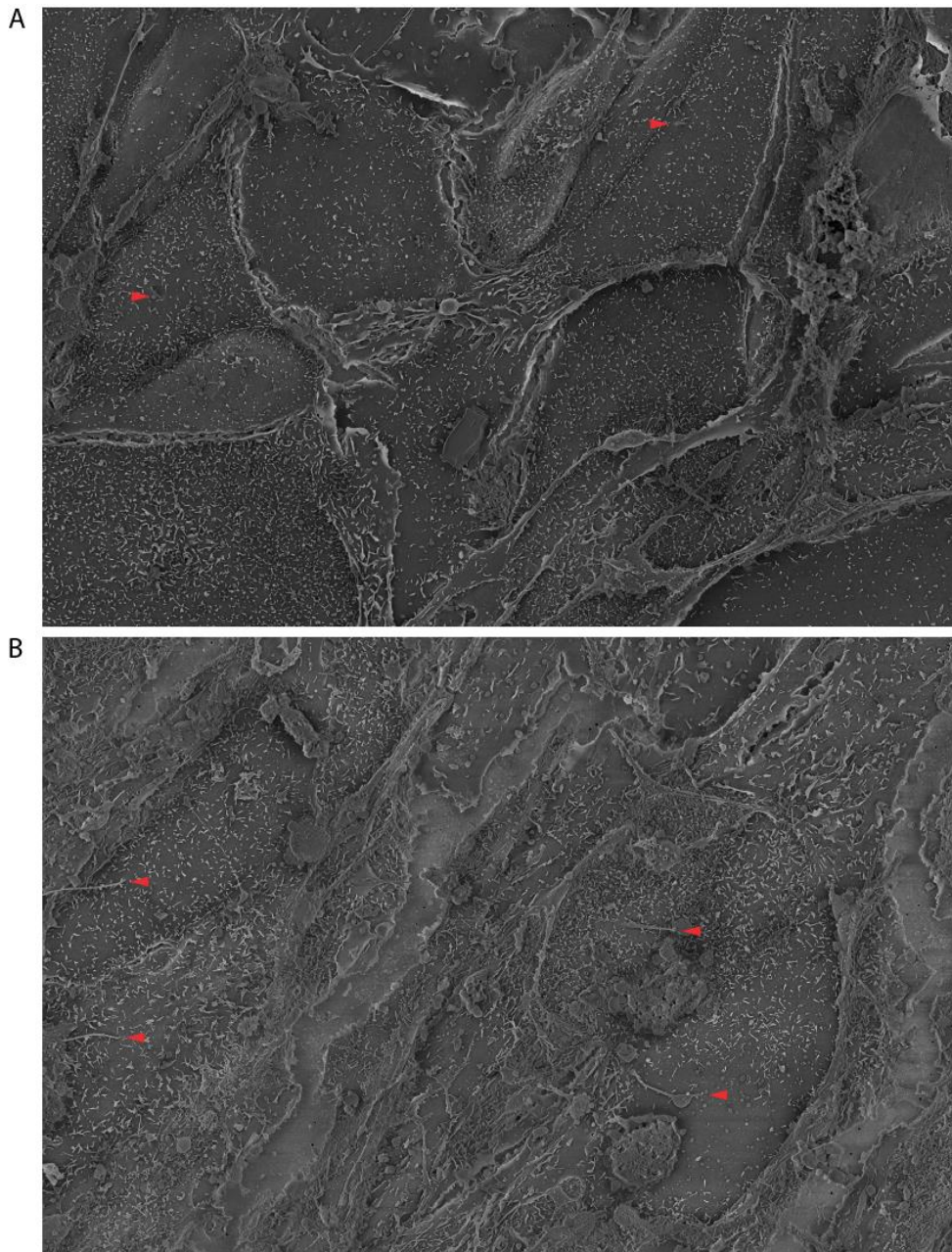


**Figure 10: SEM of RPTECs demonstrate increased number of primary cilia after differentiation**

SEM of RPTECs. **A:** Three dps, only a few cells had primary cilia (red arrows). **B:** Seven dps, more RPTECs demonstrated primary cilia-like structures (red arrows) by SEM. All images are representative images of one experiment.

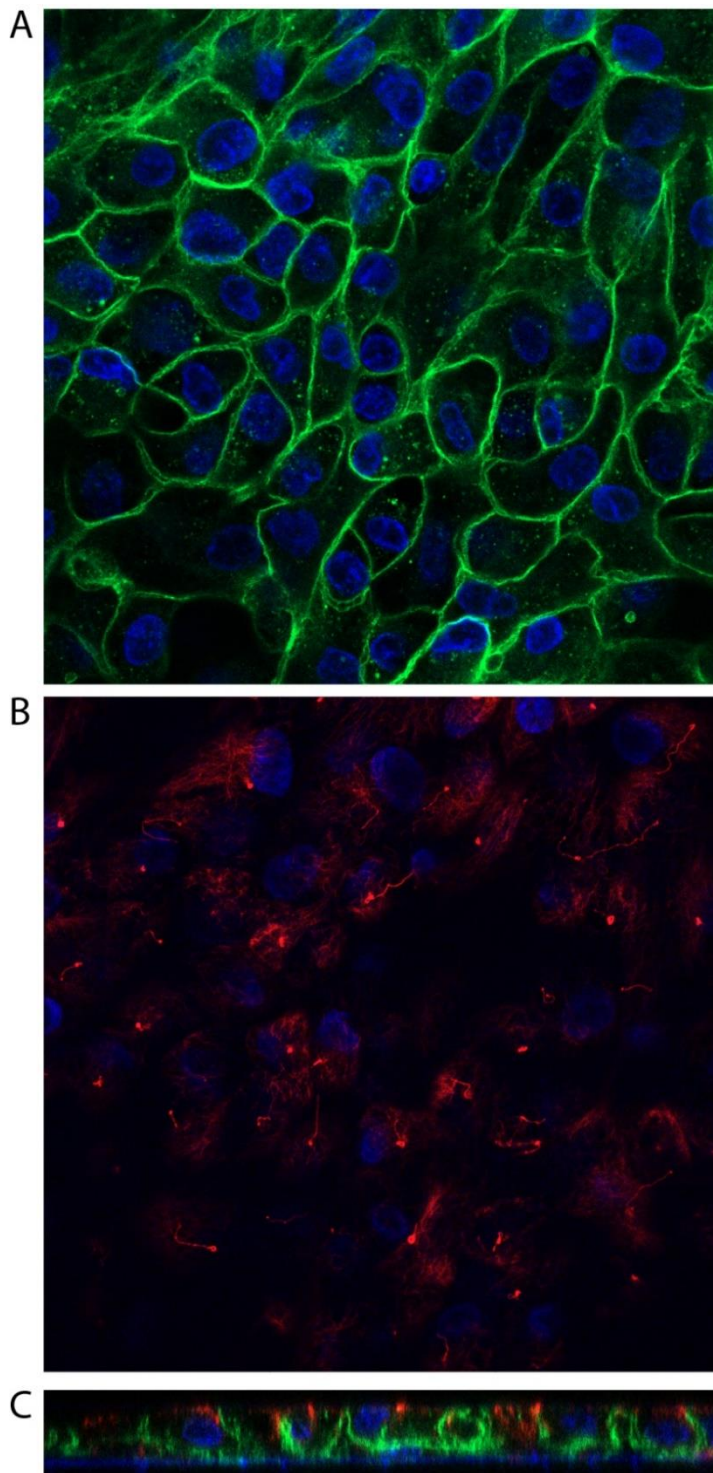


**Figure 11: RPTECs seeded upside-down develop the same polarized morphology**

IF microscopy of adult RPTECs cultured for 14 days stained for Na/K-ATPase (green) and acetylated tubulin (red) in combination with DRAQ5 (blue). **A:** Na/K-ATPase is localized in the lateral membrane. **B:** Cells exhibit punctate staining of acetylated tubulin corresponding to



primary cilia. **C:** In the lateral view, RPTECs have protruding primary cilia and basolateral Na/K-ATPase. All images are representative images of one experiment.

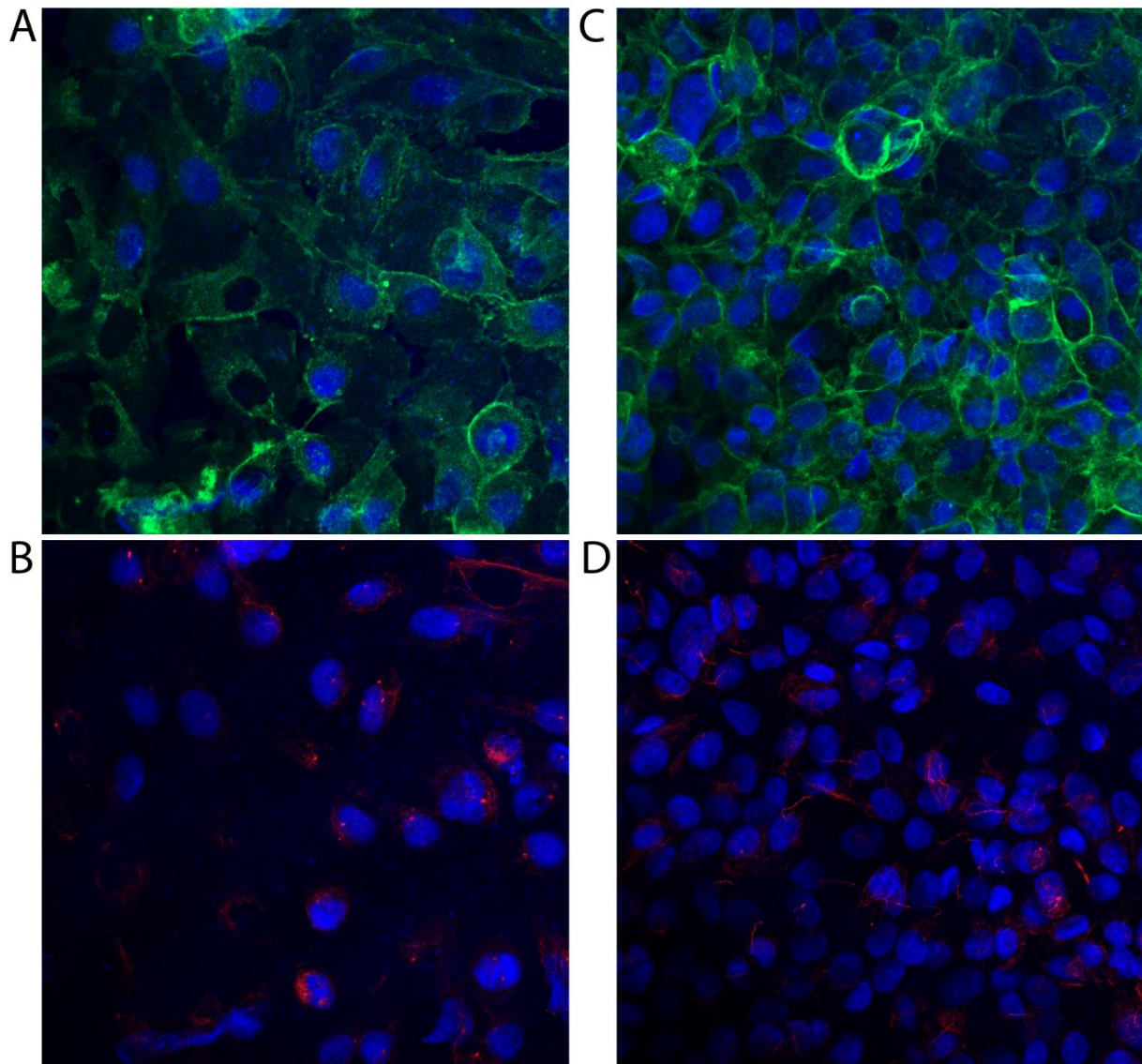


**Figure 12: RPTEC/TERT1 differentiate on permeable supports**

IF microscopy of RPTEC/TERT1s stained for Na/K-ATPase (green) or acetylated tubulin (red) in combination with DRAQ5 (blue) **A:** Three dps, RPTEC/TERT1s show diffuse staining of Na/K-ATPase. **B:** Three dps, acetylated tubulin display punctate and snaking staining of acetylated tubulin. **C:** 14 dps, Na/K-ATPase is redistributed to the lateral membrane. **D:** 14 dps, an increased number of RPTEC/TERT1s display a staining pattern of acetylated tubulin consistent with primary cilium. All images are representative images of one experiment.

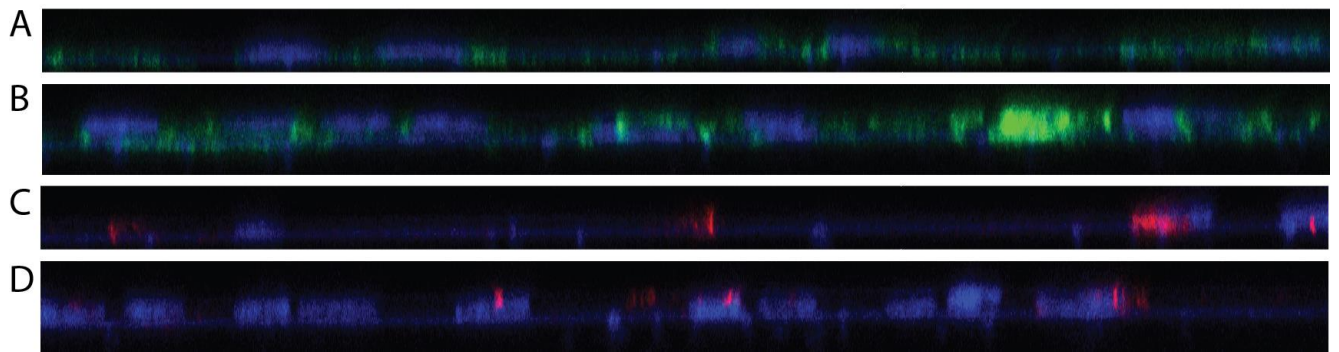


**Figure 13: Lateral view confirms polarization of RPTEC/TERT1**

Lateral view of IF microscopy of RPTEC/TERT1s stained for Na/K-ATPase (green) or acetylated tubulin (red) in combination with DRAQ5 (blue). **A:** Three dps, RPTEC/TERT1s Na/K-ATPase is diffusely distributed. **B:** Ten dps, Na/K-ATPase redistributed laterally. **C and D:** Three dps and ten dps, RPTEC/TERT1 acetylated tubulin-positive structures are protruding from the cells. All images are representative images of one experiment.

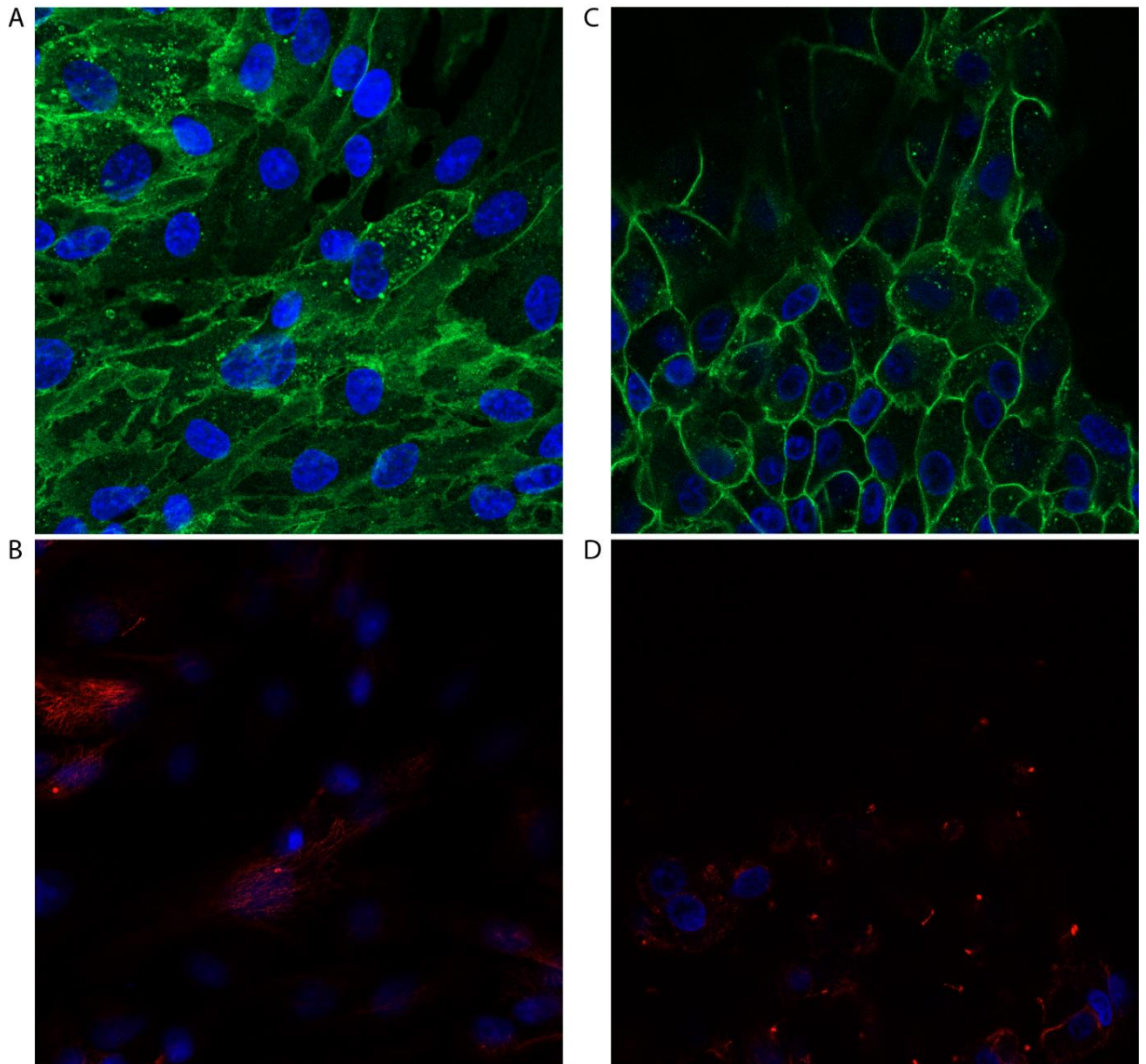


**Figure 14: RPTECs undergo polarization in chamber slides**

IF microscopy of adult RPTECs cultured in chamber slides stained for Na/K-ATPase (green) or acetylated tubulin (red) in combination with DRAQ5 (blue). **A:** Three dps, RPTEC show a diffuse and unpolarized staining of Na/K-ATPase (green). **B:** Ten dps, Na/K-ATPase is redistributed to the lateral membrane. **C:** Three dps, RPTECs have cytoskeletal staining of acetylated tubulin. **D:** Ten dps, acetylated tubulin staining is more punctate, representing primary cilia. All images are representative images of one experiment.

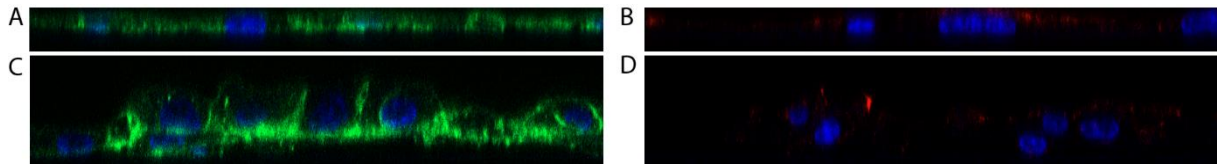


**Figure 15: RPTECs in chamber slides have basolateral Na/K-ATPase and protruding primary cilia**

Lateral view of IF microscopy of adult RPTECs cultured in chamber slides stained for Na/K-ATPase (green) or acetylated tubulin (red) in combination with DRAQ5 (blue). **A:** In the lateral view, RPTECs exhibited diffuse staining of Na/K-ATPase three dps. **B:** Ten dps, RPTECs showed strong basolateral staining of Na/K-ATPase. **C:** Three dps, few to no RPTECs had protruding acetylated tubulin-positive structures. **D:** Ten dps, a large fraction of RPTECs displayed acetylated tubulin positive structures protruding from the cell. All images are representative images of one experiment.

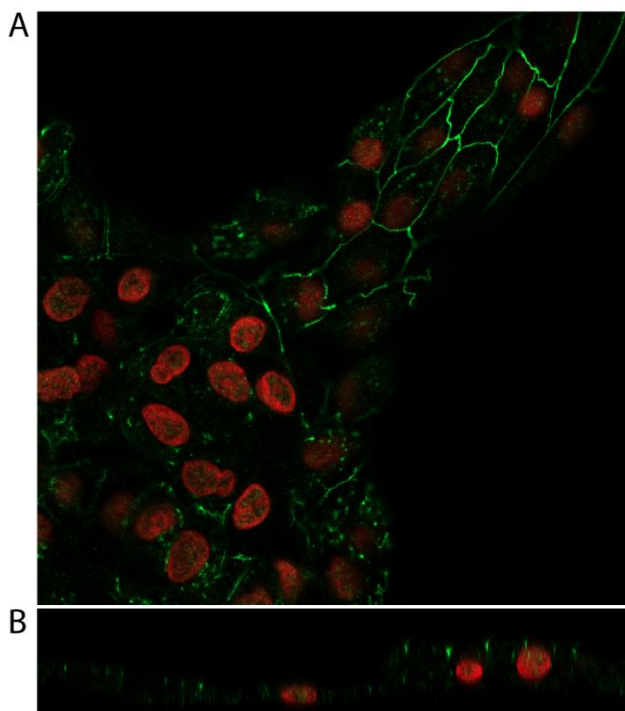


**Figure 16: RPTECs cultured in chamber slides have tight junctions**

IF microscopy of adult RPTECs cultured in chamber slides stained for Na/K-ATPase (green) and DRAQ5 (red). **A:** Ten dps, RPTEC in chamber slides showcased lateral staining of ZO-1

(green). **B:** Lateral view confirms that ZO-1 is subapically located. Images are representative images from one experiment.

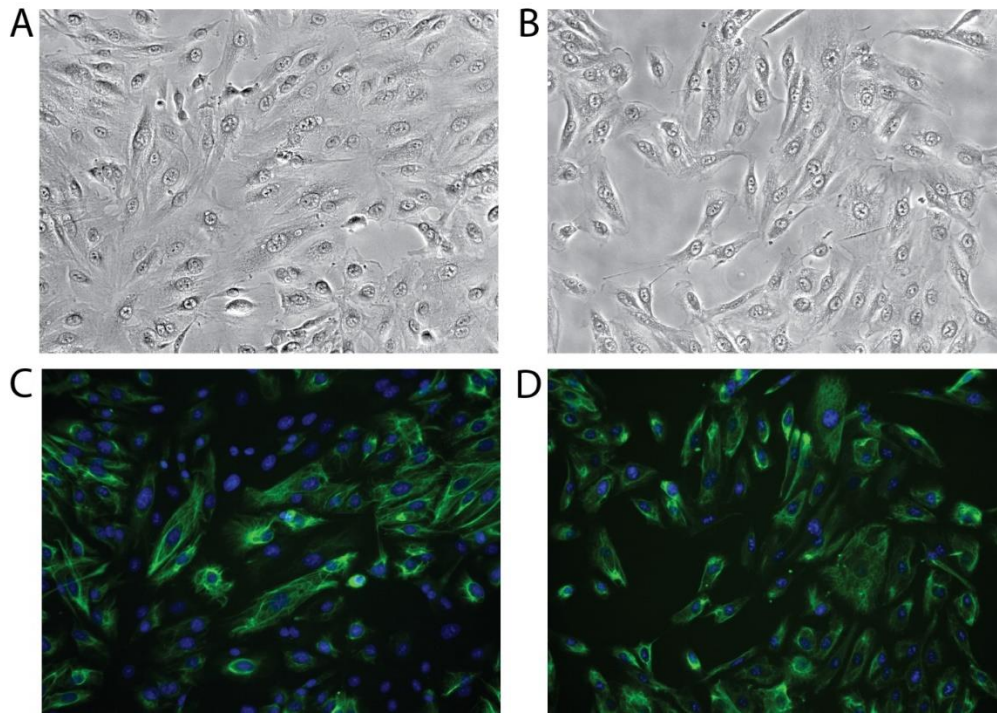


**Figure 17: Urinary cells exhibit similar morphology as RPTECs**

Phase-contrast and IF microscopy of urinary cells and adult RPTECs. Urinary cells and adult RPTECs are stained for CK-18 (green) and DRAQ5 (blue). IF microscopy **A:** Phase-contrast images of urinary cells display a elongated and oval shape. **B:** Phase-contrast images of RPTECs exhibit a shape similar to the urinary cells. **C:** IF of urinary show that urinary cells contain CK-18. **D:** RPTECs stain positive for CK-18 by IF. All images are representative images of two experiments.

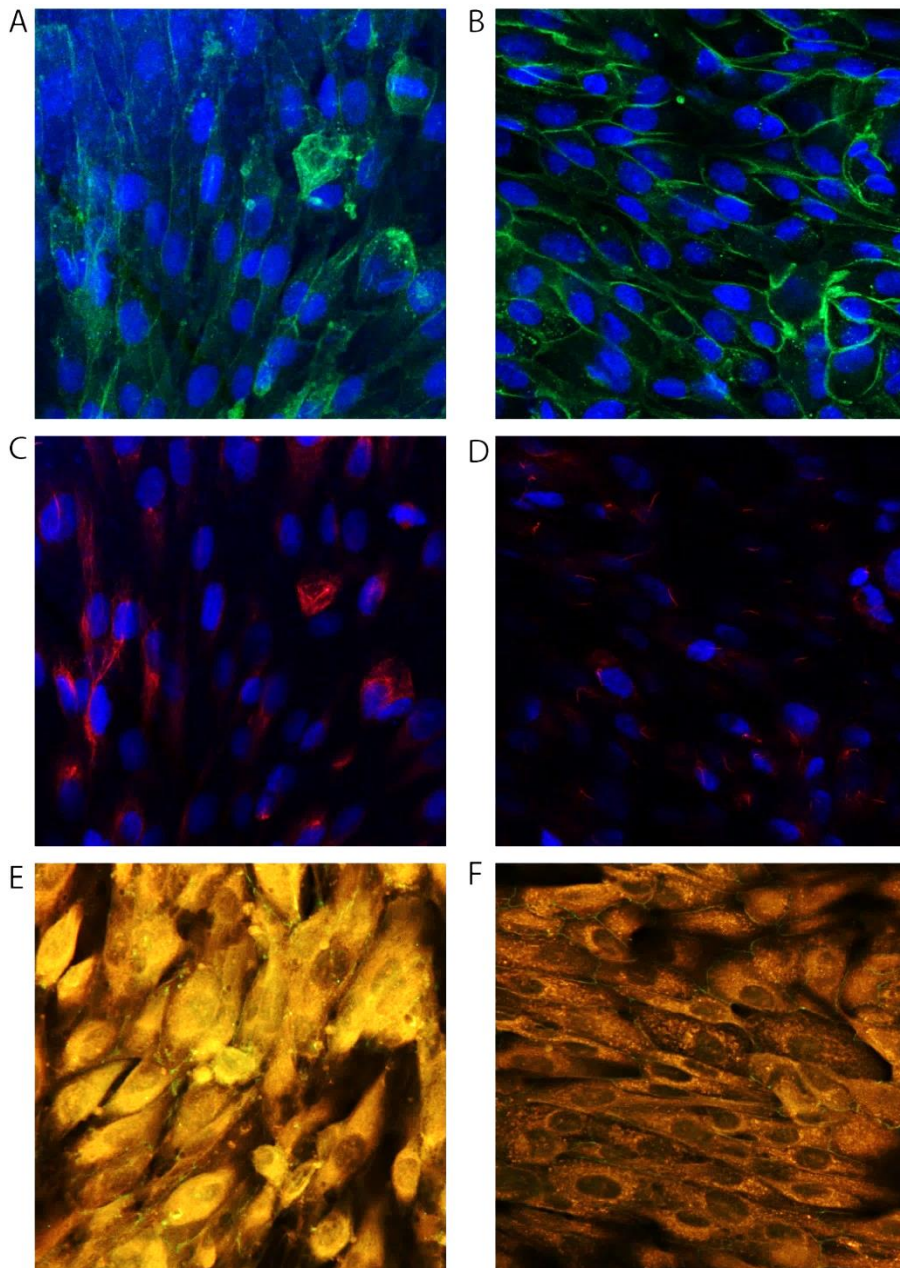


**Figure 18: Urinary cells polarize on permeable supports**

IF microscopy of urinary cells stained for Na/K-ATPase (green) or acetylated tubulin (red) in combination with DRAQ5 (blue) or stained for ZO-1 (green) in combination with the membrane marker CellMask (orange). **A:** Three dps, Na/K-ATPase was diffusely distributed in urinary cells. **B:** 14 dps, Na/K-ATPase had been redistributed to the lateral membrane. **C:** Three dps, urinary cells displayed cytoskeletal staining pattern of acetylated tubulin. **D:** 14 dps, acetylated tubulin displayed a more punctate staining. **E:** Three dps, urinary cells display ZO-1 (green) staining between cells. **F:** 14 dps, urinary cells display increased expression of ZO-1 between cells. All images are representative images of one experiment.

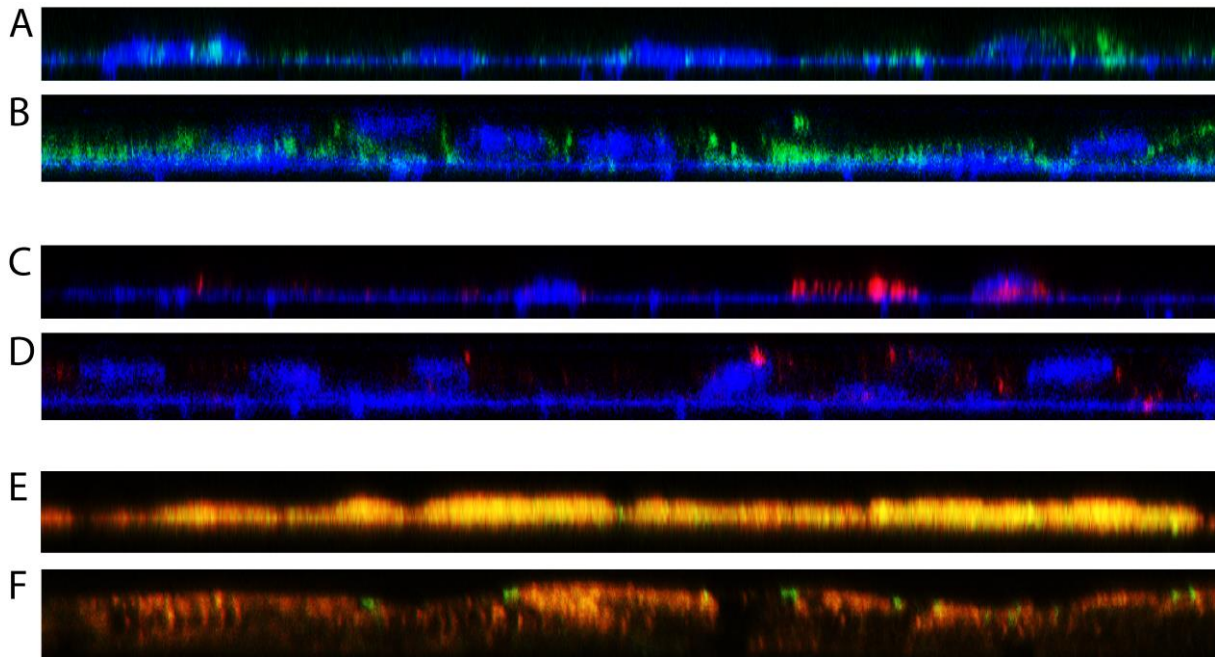


**Figure 19: Differentiation leads to basolateral Na/K-ATPase, primary cilium and tight junctions.**

Lateral view of IF microscopy of urinary cells stained for Na/K-ATPase (green) or acetylated tubulin (red) in combination with DRAQ5 (blue) or stained for ZO-1 (green) in combination with the membrane marker CellMask (orange). **A:** Three dps, Na/K-ATPase was diffusely distributed in the entire cell. **B:** 14 dps, Na/K-ATPase exhibited strong basolateral expression. **C:** Three dps, urinary cells did not have any protruding primary cilia. **D:** 14 dps, urinary cells developed protruding structures that stain positive for acetylated tubulin. **E:** Three dps, urinary cells had ZO-1 in the lateral membranes. **F:** 14 dps, ZO-1 was more subapically located compared to three dps. All images are representative images of one experiment.

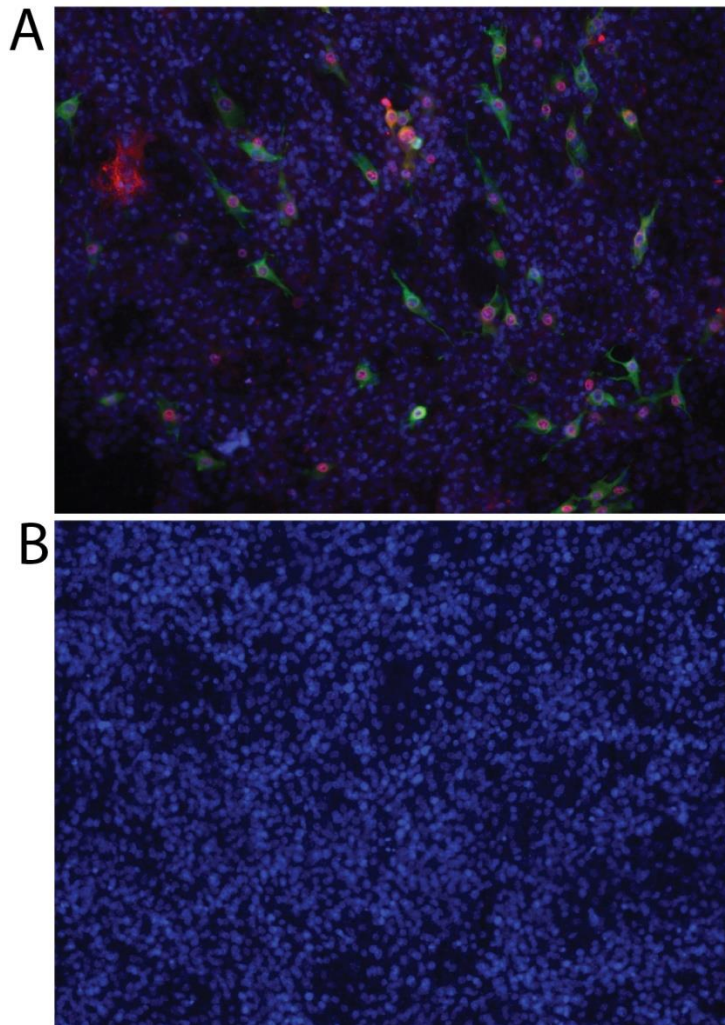


**Figure 20: Polarized RPTECs supports BKPyV infections**

IF microscopy of adult RPTECs stained for agnoprotein (green), VP1 (red) and DRAQ5 (blue).

**A:** 14 dps, RPTECs were infected with BKPyV and three days post infection (17 dps) cells were stained for BKPyV agnoprotein and VP1. **B:** Mock infected RPTECs stained for agnoprotein and VP1 did not exhibit any staining. All images are representative images of two experiments.



<p><b>Reference:</b> Van der Hauwaert C, Savary G, Gnehm V, Glowacki F, Pottier N, Bouillez A, et al. Isolation and characterization of a primary proximal tubular epithelial cell model from human kidney by CD10/CD13 double labeling. <i>PLoS One</i>. 2013;8(6):e66750-e.</p>		<p><b>Design:</b> Experimental study</p>

Aim	Materials and methods	Results	Discussion/comments
<p>The aim of the study was to develop a new, more homogenous cell culture model of proximal tubular epithelial cells from kidney tissue.</p>	<p>Cells were isolated from fresh kidney tissue from nephrectomies. Fluorescence activating cell sorting was used to further isolate proximal tubular epithelial cells. Cells were cultured in Boyden chambers with collagen IV, Matrigel or without matrix or in Lab-Tek chambers.</p>	<ul style="list-style-type: none"> <li>- All cell populations expressed epithelial markers.</li> <li>- CD10 or CD13 positive cells exhibited a heterogeneous cell population that expressed markers of both the proximal tubule and the distal tubule.</li> <li>- CD10/CD13 positive cells only expressed markers of proximal tubular epithelial cells by western blotting, immunofluorescence microscopy and reverse transcriptase PCR.</li> <li>- Both CD10/CD13-positive and CD10/CD13 negative cells exhibited a polarized ultrastructure.</li> <li>- Alkaline phosphatase activity was higher in CD10/CD13 positive cells than CD10/CD13 negative cells.</li> </ul>	<p>The study present a method for isolating proximal tubular epithelial cells from kidney tissue. The cells are extensive characterization of the morphology and functionality makes the findings convincing.</p> <p><b>Strengths and weaknesses of the study:</b></p> <p><b>Strengths:</b></p> <ul style="list-style-type: none"> <li>- Extensive characterization of the isolated cells by multiple methods validates the origin of the cells</li> <li>- Results of different methods support each other.</li> </ul> <p><b>Weaknesses:</b></p> <ul style="list-style-type: none"> <li>- Immunofluorescence microscopy was not performed on cells cultured on permeable supports.</li> <li>- Polarity was not assessed by immunofluorescence microscopy, only electron microscopy. Confocal Z-stacks are suitable for investigating if polarity markers are distributed in a polarized manner.</li> </ul> <p><b>Do the authors reference other literature that strengthen/weaken their results?</b></p> <ul style="list-style-type: none"> <li>- Yes, the polarity markers used are extensively referenced in the scientific literature.</li> <li>- CD10 and CD13 as markers of proximal tubular epithelial cells is referenced.</li> </ul>
<p><b>Conclusion</b></p> <p>The study describes a method for establishing a homogenous and robust cell culture model for proximal tubular epithelial cells. CD10/CD13 positive cells represent proximal tubular epithelial cells.</p>	<p>Polarity was assessed by immunofluorescence microscopy, western blot, electron microscopy, measuring transepithelial resistance, reverse transcriptase PCR and by the alkaline phosphatase assay.</p>		
<p><b>Country</b></p> <p>France</p>			
<p><b>Year</b></p> <p>2013</p>			

**Reference:** Schlutgens F, Rookmaaker MB, Margaritis T, Rios A, Ammerlaan C, Jansen J, et al. Tubuloids derived from human adult kidney and urine for personalized disease modeling. *Nat Biotechnol.* 2019;37(3):303-13.

		<b>Design: Experimental study</b>	
<b>Aim</b>	<b>Materials og methods</b>	<b>Results</b>	<b>Discussion/comments</b>
<p>The aim of the study was to develop a polarized epithelial organoid culture of renal epithelial cells (tubuloids).</p>	<p>The study utilizes a variety of techniques such as cell culture, immunofluorescence microscopy, electron microscopy, whole genome sequencing, single cell sequencing and infection studies.</p>	<ul style="list-style-type: none"> <li>- Tubuloids can be established from kidney biopsies and urine.</li> <li>- Tubuloids are of renal origin – they express renal markers, and exhibit functionality similar to the proximal tubule.</li> <li>- Tubuloids are permissive for BK Polyomavirus, can support productive infection and can be used to model infection of BK Polyomavirus.</li> <li>- Tumorioids can be established from nephroblastoma-tissue.</li> <li>- The tumorioids develop a differing morphology from healthy tubuloids and exhibit known morphologic traits and mutations of nephroblastoma.</li> <li>- Tubuloids can be established from the urine of patients with cystic fibrosis. CF-tubuloids exhibit morphological traits similar to those described in enteroids isolated from a CF-patient. The forskolin-swelling assay also model treatment response in tubuloids.</li> <li>- Tubuloids can be cultured in OrganoPlates</li> </ul>	<p>Overall, the paper is very convincing and solid scientific work. The authors describe a novel and useful cell culture and provide convincing evidence that the cell culture model. The use of multiple methods, thorough assessment of polarity and modelling of three different kidney conditions showcase the relevance of the tubuloid model.</p> <p><b>Strengths and weaknesses of the study:</b></p> <p><b>Strengths:</b></p> <ul style="list-style-type: none"> <li>- Extensive characterization of the tubuloid culture using several different methods. The method is also quick and easier compared to other organoid cultures.</li> <li>- The authors use known markers and assays to assess if the cell culture is polarized</li> <li>- Renal epithelial cells are isolated by two different methods</li> <li>- The authors prove the relevance of the model by modelling several different diseases affecting the kidneys</li> </ul> <p><b>Weaknesses:</b></p> <ul style="list-style-type: none"> <li>- The screening of tubuloids for BK Polyomavirus could have been described better</li> <li>- CF-tubuloids only established from one patient</li> <li>- The tubuloids is less complex compared to iPSC-derived kidney organoids.</li> </ul> <p><b>Do the authors reference other publications?</b></p> <p>Yes. The publication references previous work of the authors on similar organoids derived from different tissues such as enteroids. They also reference numerous other publications that support their choice of polarity markers.</p>
<p><b>Conclusion</b></p> <p>Tubuloids is a novel and relevant cell culture system of renal tubular epithelial cells. The tubuloid can be used to model infectious diseases, cancer and cystic fibrosis.</p>	<p>In addition, the authors also use several established assays for examining known traits of polarized epithelial cells namely the barrier integrity assay, P-glycoprotein assay and rhodamine-123-assay.</p>		
<p><b>Country</b></p> <p>Netherlands</p>			
<p><b>Year</b></p> <p>2019</p>			

**Reference:** Krautkrämer E, Lehmann MJ, Bollinger V, Zeier M. Polar release of pathogenic Old World hantaviruses from renal tubular epithelial cells. *Virology*. 2012;9(1):299.

**Design:** Experimental study

Aim	Materials and methods	Results	Discussion/comments
<p>The aim of the study was to investigate if pathogenic Old World hantaviruses is released in a polarized manner.</p>	<p>Cells: Vero C1008, primary human renal epithelial cells and Madin-Darby Canine kidney cells. Polarized cells were passaged on permeable supports.</p> <p>Virus: Hantaan and Puumala virus</p>	<ul style="list-style-type: none"> <li>- MDCK cells express the hantavirus receptor CD55 and integrin <math>\alpha V\beta_3</math>.</li> <li>- Vero C1008, primary renal epithelial cells and MDCK cells supported Hantavirus-infection.</li> <li>- Hantaviruses entered MDCK cells from the apical surface</li> <li>- Hantavirus progeny virus was released from the apical surface.</li> </ul>	<p>The study provide evidence that Old World Hantaviruses exhibit polarized release in polarized epithelial cells. The study show that both Hantaan and Puumala Hantavirus is released exclusively from the apical surface in three relevant polarized epithelial cells and cell lines. Drawbacks are that the polarity of the cells is assessed or referenced sufficiently, release is not directly quantitated and they did not perform immunofluorescence microscopy of MDCK against integrin <math>\alpha V\beta_3</math> and CD55.</p> <p><b>Strengths and weaknesses of the study:</b></p> <p><b>Strengths:</b></p> <ul style="list-style-type: none"> <li>- The study utilizes to hantaviruses, increasing the relevance of the findings.</li> <li>- The investigators have assessed release in three types of polarized epithelial cells, including primary human renal epithelial cells.</li> </ul> <p><b>Weaknesses:</b></p> <ul style="list-style-type: none"> <li>- Assessment of polarity is only done for MDCK cells. The authors present no evidence that Vero C1008 or primary renal epithelial cells polarize.</li> <li>- The presence of hantavirus-receptors is only done with flow cytometry. Immunofluorescence microscopy of MDCK cells could reveal if the localization of the receptor is restricted to a specific cell surface. This is important information as it will impact if viral entry is polarized or not.</li> <li>- The authors did not directly quantitate the release of progeny virus. In my opinion this is important information and could be done by RT-PCR.</li> <li>- The paper does not address if the membrane of the permeable support poses as a mechanical barrier for the virus. This is an essential point, as basolateral release can potentially be hindered by the membrane and thereby falsely reduce basolateral release of progeny virus.</li> </ul> <p><b>Do the authors reference other literature that strengthen/weaken their results?</b></p> <ul style="list-style-type: none"> <li>- Yes, the authors reference their previous findings that viral entry of Old World Hantavirus is restricted to the apical surface. Additionally, they also reference previous work from Ravkov et al. where they showed that viral entry and release of New World Hantavirus is restricted to the apical surface.</li> </ul>
<p><b>Conclusion</b></p>	<p>Infectivity was assessed by western blot and immunofluorescence microscopy.</p>		
<p>Release of Pathogenic Old World hantaviruses is polarized in polarized renal epithelial cells.</p>			
<p><b>Country</b></p>	<p>Germany</p>		
<p><b>Year</b></p>	<p>2012</p>		

**Reference:** Vinaiphath A, Channakraw K, Thongboonkerd V. More complete polarization of renal tubular epithelial cells by artificial urine. *Cell Death Discov.* 2018;4(1):47.

**Design:** Experimental study

Aim	Materials and methods	Results	Discussion/comments
<p>To assess if artificial urine in the apical compartment yields more complete polarization of renal tubular epithelial cells.</p>	<p>Cells: Madine-Darby Canine Kidney cells. The presence of polarity markers was assessed by transepithelial I resistance, immunofluorescence microscopy, electron microscopy and western blot. The functionality of the monolayer was examined by utilizing an ion transport assay and lactate dehydrogenase release assay.</p>	<ul style="list-style-type: none"> <li>- Culture with artificial urine in the apical compartment lead to increased expression of polarity markers such as tight junctions, adherens junctions, microvilli and desmosomes.</li> <li>- Electron microscopy showed that MDCK cells cultured with artificial urine developed a more polarized ultrastructure.</li> <li>- The secretome of MDCK cells cultured in artificial urine was more similar to the secretome of human urine compared to control-MDCK cells.</li> <li>- Urea is the main driver in artificial urine of more complete polarization.</li> </ul>	<p>The paper show in a convincing manner how artificial urine lead to more complete polarization of MDCK cells. Utilization of several methods, assessment of morphology and functionality and the use of established polarity markers make the findings convincing.</p> <p><b>Strengths and weaknesses of the study</b></p> <p><b>Strengths:</b></p> <ul style="list-style-type: none"> <li>- Polarity was assessed by multiple modalities such as immunofluorescence and electron microscopy, transepithelial resistance and western blot.</li> <li>- MDCK cells is an established and relevant cell line in research of epithelial cell polarization.</li> <li>- Secretome analysis showcase the impact polarization has on the functionality of the monolayer.</li> </ul> <p><b>Weaknesses:</b></p> <ul style="list-style-type: none"> <li>- The study only utilizes MDCK cells. Although MDCK cells is an established and relevant cell culture model of polarized epithelial cells it would strengthen the paper if the findings were reproducible in other kidney cells lines or primary renal epithelial cells.</li> </ul> <p><b>Do the authors reference other literature that strengthen/weaken their results?</b></p> <ul style="list-style-type: none"> <li>- Yes, the polarity markers in the study is well-established and referenced in the scientific literature. The authors also reference previous papers that have also shown that hyperosmotic conditions lead to changes in gene expression and cell morphology.</li> </ul>
<p><b>Conclusion</b></p>	<p>Culture of renal tubular epithelial cells with artificial urine yields a more complete polarization. Urea is the most important facilitator of polarization in artificial urine.</p>		
<p><b>Country</b></p>	<p>Thailand</p>		
<p><b>Year</b></p>	<p>2018</p>		

**Reference:** Clayson ET, Compans RW. Entry of simian virus 40 is restricted to apical surfaces of polarized epithelial cells. Mol Cell Biol. 1988;8(8):3391-6.

**Design:** Experimental study

Aim	Materials and methods	Results	Discussion/comments
<p>The aim of the study was to assess if uptake of Simian Virus 40 is polarized or not in polarized epithelial cells.</p>	<p>Cells: Vero C1008, polarized MDCK, primary African green monkey kidney cells, Vero and CV-1. Cells were grown on permeable supports.</p> <p>Virus binding was assessed by electron microscopy, immunofluorescence microscopy and liquid scintillation spectrometry.</p>	<ul style="list-style-type: none"> <li>- Binding of Simian Virus 40 was restricted to the apical side of polarized epithelial cells.</li> <li>- In non-polarized epithelial cells, Simian Virus 40-binding was non-polarized.</li> <li>- Polarized epithelial cells infected from the basal side did not express viral proteins, while polarized cells infected from the apical side expressed virus proteins.</li> </ul>	<p>The paper present evidence of polarized entry of Simian Virus 40 in polarized epithelial cells. Virus binding and infectivity results harmonize making the evidence convincing. The authors have utilized both cell lines and primary cells, but the polarity of the cell culture model is poorly documented.</p> <p><b>Strengths and weaknesses of the study:</b></p> <p><b>Strengths:</b></p> <ul style="list-style-type: none"> <li>- Virus uptake was assessed in both polarized and non-polarized epithelial cells. Authors utilized two polarized cell lines and two non-polarized cell lines.</li> <li>- Utilized both primary cells and immortalized cell lines.</li> <li>- Infection and site of entry is assessed by several methods strengthening the evidence. Results of different methods harmonize.</li> </ul> <p><b>Weaknesses:</b></p> <ul style="list-style-type: none"> <li>- The polarized epithelial cells are not thoroughly assessed for polarity markers and functionality. No convincing evidence that confirm the polarity of the cells used in the study.</li> <li>- The authors do not address if the membrane of the permeable support act as a mechanical barrier. This is a drawback as other studies have shown that the membrane acts as a barrier the virus must cross.</li> </ul> <p><b>Do the authors reference other literature that strengthen/weaken their results?</b></p> <p>Yes, the authors reference other papers where polarized entry and release have been shown in other viruses.</p>
<p><b>Conclusion</b></p> <p>The uptake of Simian Virus 40 is polarized and restricted to the apical surface of polarized epithelial cells</p>			
<p><b>Country</b></p> <p>USA</p>			
<p><b>Year</b></p> <p>1988</p>			